SOLUTION TREATMENT AND AGING CHARACTERISTICS OF THERMOMECHANICALLY TREATED 18 Ni 250 MARAGING STEEL

A Thesis Submitted

In Partial Fulfilment of the Requirements

for the Degree of

MASTER OF TECHNOLOGY

by

VISHAL DIKSHIT

to the

DEPARTMENT OF MATERIALS AND METALLURGICAL ENGINEERING

INDIAN INSTITUTE OF TECHNOLOGY, KANPUR

June 1994

MME - 1994 - M - DIK - SOL

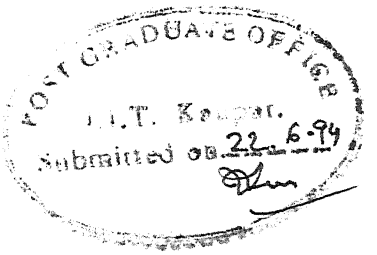

C E R T I F I C A T E

It is certified that the work contained in the thesis entitled "Solution Treatment and Aging Characteristics of Thermomechanically Treated 18 Ni 250 Maraging Steel" by Vishal Dikshit, has been carried out under our supervision and that this work has not been submitted elsewhere for a degree.

Dr. S. Bhargava
Associate Professor

Dr. S. Sangal
Assistant Professor

Department of Materials and Metallurgical Engineering
Indian Institute of Technology, Kanpur

June 1994

CONTENTS

ACKNOWLEDGEMENTS

I am very thankful to my project guides Dr. S. Bhargava and Dr. S. Sangal for their cooperation in my project work. Their subject knowledge and keen analysis of the topic helped me a lot. The valuable suggestions extended by them during the course of the project enabled me to come up triumphant in this endeavour.

I wish to express my deepest gratitude to the faculty members of the department of Materials and Metallurgical Engg. for providing me with the laboratory facilities for conducting my investigation.

I am also thankful to the following persons:

Mr. K.P. Mukerji, Mr. V.P. Gupta, Mr. Mungole, Mr. A.K. Awasthi, Mr. Satyam Suwas and Mr. A.K. Srivastava for their help in my project work.

VISHAL DIKSHIT

LIST OF TABLES

LIST OF FIGURES

LIST OF ABBREVIATIONS

AR	As received sample from Midhani
SS	Single Solutionised
DS	Double Solutionised
TMT	Thermomechanical Treatment
EE	Electrolytic Etching
CE	Chemical Etching
SEM	Scanning Electron Micrograph

ABSTRACT

Two different types of solutionising treatments namely single solutionising and double solutionising were employed on thermomechanically treated 18Ni 250 maraging steel. Static strain aging behaviour of the solutionised steel was studied. Mechanical properties of the aged steel subjected to different solutionising treatments were analysed. It was found that although the general trend in variation of properties of differently solutionised steels was same, single solutionising proved to be advantageous at lower temperatures of aging.

Microstructural observations were carried out to investigate the effect of thermomechanical treatment and aging on the microstructural features of 18Ni 250 maraging steel. Fractured surface of the steel was also seen under scanning electron microscope. Typical lath martensite structure and intercrystalline brittle fracture was seen.

CHAPTER - 1

INTRODUCTION

Maraging steels are ultra high strength steels generally containing nickel, molybdenum, cobalt, titanum, aluminium and a very low percentage of carbon [C ≤ 0.03%].

There are basically four wrought commercial maraging steels of the 18 per cent nickel family and one cast grade. The compositions and nominal 0.2 per cent yield strength values are presented in Table 1.1. Yield strength of maraging steels varies from 1030 to 2420 MPa (150 to 350 Ksi). Some experimental [1] maraging steels have yield strength as high as 3450 MPa (500 Ksi).

The precipitation of intermetallic phases based on substitutional alloying elements with in the matrix of iron nickel martensite [1] is responsible for the strengthening effect during aging of these steels. Precipitates which form in maraging steels are based on intermetallic compositions and are not carbides as in HSLA steels. Hence carbon in maraging steels is treated as an impurity and is kept at the lowest possible concentration. Carbon, if present, causes embrittlement of the steel by forming titanium carbides or carbonitrides [1]. The term `maraging' is an abbreviation of `martensite age hardening'.

The use of intermetallic precipitates to achieve strengthening provides several unique characteristics to maraging steels that set them apart from conventional steels. Hardenability is of no concern because of high Ni content and low carbon content. Toughness is enhanced because there is no pinning [2] of dislocations by carbon. Also the low carbon martensite

TABLE 1.1

Nominal chemical composition and strengths of common maraging steels

Maraging steel type	Nominal composition, wt %*							Nominal yield strength (MPa)
	Ni	Co	Mo	Al	Ti	Cr	C(max)	
18 Ni 200	18	8.5	3.2	0.1	0.2	-	0.03	1378
18 Ni 250	18	8.0	4.8	0.1	0.4	-	0.03	1722
18 Ni 300	18.5	8.75	5.0	0.1	0.6	-	0.03	2067
12-5-3	12.0		3.0	0.4	0.2	5.0	0.03	1240
Cast 17 Ni	17.0	10.25	4.6	0.1	0.3	-	0.03	1619

*Balance material in all the compositions is Fe.

soft, about 30 to 35 HRC. During age hardening there is only a very slight dimensional change. Thus fairly intricate shapes can be machined [3] in soft condition and then hardened with minimum of distortion.

1.1 CHARACTERISTIC PROPERTIES OF MARAGING STEELS

1. The chief property making maraging steels so interesting as a structural material is their excellent [1] combination of strength and fracture toughness.

2. Maraging steels possess reasonably good mechanical properties at elevated as well as at low temperatures. Although the fracture toughness values (K_{IC}) sometimes decreases by ~ 60% when the temperature is lowered from room temperature to -194°C the combination of strength with toughness is [1] still rather good over a wide range of low temperatures which makes these steels highly attractive for cryogenic applications. The high temperature capability of these steels is generally limited to 480°C.

3. The fatigue properties of these steels are generally comparable to those of high strength alloyed steels.

4. 18 Ni maraging steels generally offer better threshold plane strain stress intensity values (K_{ISCC}) than other high strength steels. In terms of critical crack size, maraging steels can tolerate larger flaws without experiencing crack propagation.

5. Embrittlement resistance of maraging steels when compared to that of plain carbon and alloy steels is generally found to be superior. Some of the typical features of maraging steels in this regard have been shown in Table 1.2. [2].

TABLE 1.2

Type of embrittlement	Steel		
	C and alloy steels	18 Ni 300 maraging	12-5-3 maraging
HOT HYDROGEN			
CVN after 1000 hrs at 454°C in 1000 psi H_2	<13.35* J	-	42.72 J
CATHODIC CHARGING HYDROGEN			
Tensile Reduction of area after charging for 10 minutes at 0.02 amp/sq.inch in 4% H_2SO_4 saturated by NaCN	3%*	42%	-
Baking time at 149°C required to restore ductility of severely embrittled specimens	20 hrs*	2 hrs	-
NEUTRON RADIATION			
Increase of transition temperature with 3×10^{19} n/cm^2(>1Mev) irradiation	121°C	-	20°C
TEMPER			
CVN after 10,000 hrs at 454°C	<13.35 J*	-	53.4 J

*Quenched and aged.

1.2 Applications

The uses of conventional 18% Ni maraging steels can be classified into three major groups:

(a) Hydrospace, aeronautical and aerospace applications- rocket motor cases, torsion bar suspensions for space vehicles, parts of missile engines, aircraft landing gear components, submergence marine vehicles for great depths etc.

(b) Structural and machine components - pressure vessels, bolts, fasteners, springs, barrels for rapid firing guns, fuel injection pumps, etc.

(c) Tools - diecasting dies, moulds for plastic industry, some cold forming dies, etc. [1].

1.3 PHASE TRANSFORMATIONS IN MARAGING STEELS

1.3.1 Martensite Formation

As mentioned earlier, maraging steels derive their ultra-high strength from a structure which consists of a martensite matrix having uniformly distributed fine precipitates of intermetallic phases.

The formation of martensite in maraging steels can be directly related to the iron-rich end of the Fe-Ni phase diagram which is shown in Figure 1.1. The low temperature equilibrium phases in the Fe rich alloys are either ferrite (at concentrations of < 10 wt% Ni) or ferrite and austenite (at concentrations of 10 wt% $<$ Ni $<$~33 wt%). Above ~ 33 wt% of Ni only austenite is present at room temperature.

Detailed studies on Fe-Ni alloys, however, reveal that a surprising variety of transformation reactions can take place in

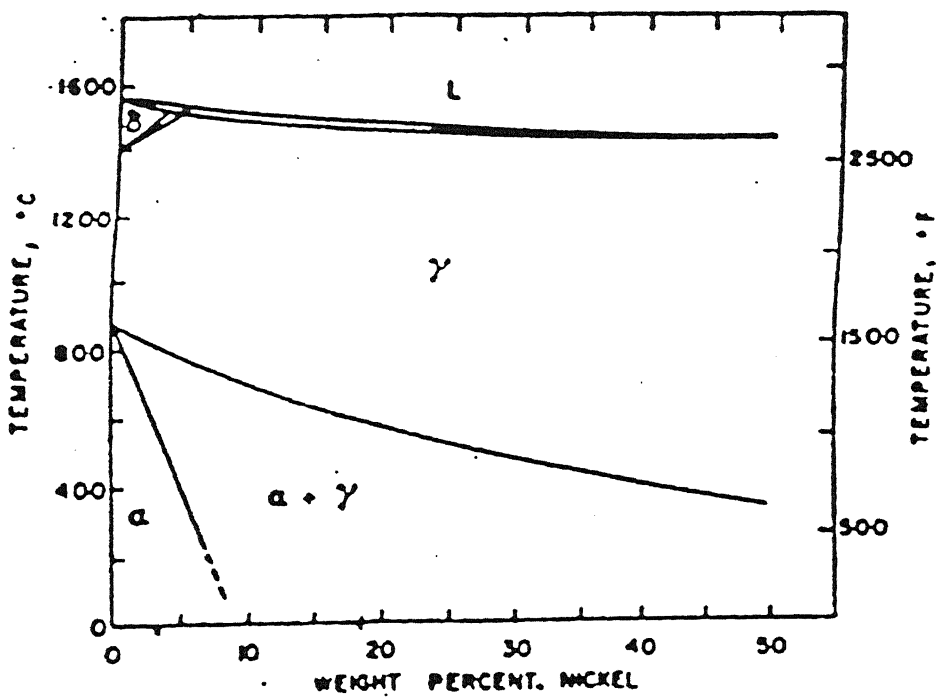

[Courtesy Iron Steel Insl.

FIG1.1 Iron-rich portion of the iron–nickel equilibrium diagram. (*Owen and Liu.*[8])

these alloys [1]. In the range of 0-5 wt% Ni alloys, ferrite forms independent of the cooling rate. In alloys containing 5-10 wt% Ni, ferrite forms when the transformation is carried out at slower cooling rate but with an increase in cooling rate the transformation product becomes martensite instead of ferrite. Increasing Ni content further lowers the cooling rate necessary to form martensite [1].

Therefore, in maraging steels, which contain ~ 18 wt% Ni, high temperature austenitic phase does not transform into equilibrium phases as predicted by the Fe-Ni phase diagram (Figure 1.1). Instead even at slow cooling rate austenite transforms to martensite which has a bcc structure. The martensite start temperature, M_s, in Fe-Ni alloys depends on the Ni content of the alloy - the higher the Ni content lower is the M_s temperature.

There exists a `thermal hysteresis' in Fe-Ni alloys between the formation of martensite on cooling and its reversion to austenite on heating [4]. This thermal hysteresis is depicted in Figure 1.2. Due to relatively higher Ni content and low carbon content in maraging steels, their hardenability is generally independent of cooling rate and the alloys are usually cooled in air.

1.3.2 Morphological Features of Martensite in Maraging Steels

Martensites in Fe - 10-25% Ni alloys possess the lath morphology . Martensites in alloys containing > 25 wt% Ni have been found to have `twinned' structure. The precise conditions that determine whether lath or twinned martensite is formed are still uncertain, but two factors seems to play a dominant role viz

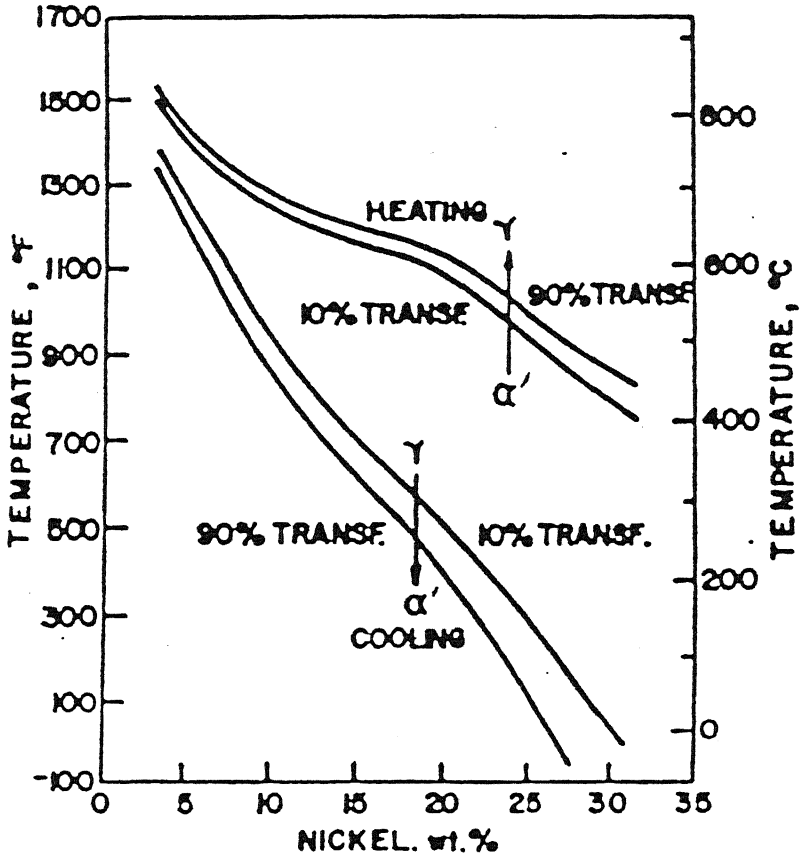

FIG.1.2 Metastable Iron-Nickel Phase Diagram.

the M_s temperature and stacking fault energy. A decrese in M_s temperature and an increase in stacking fault energy (SFE) favour the formation of twinned martensite [1]. The M_s temperature can be modified either by changes in the composition or by plastic deformation while the SFE varies only as a result of alloying.

The orientation relationship between martensite platelets and austenite matrix has been suggested to be Kurdiumov-Sachs (K-S) [1].

$$\left.\begin{array}{l} (111)_\gamma \parallel (011)_{\alpha'} \\ [1\bar{1}0]_\gamma \parallel [1\bar{1}1]_{\alpha'} \end{array}\right\} \text{[K-S]}$$

The simultaneous existence of the Kurdiumov- Sacks and the Nishiyama-Wasserman (N-W) orientation relationships has also been reported [3].

$$\left.\begin{array}{l} (111)_\gamma \parallel (011)_{\alpha'}; \\ [100]_\gamma \parallel [100]_{\alpha'} \end{array}\right\} \text{[N-W]}$$

Morphology and microstructures of lath martensites in Fe-Ni alloys and maraging steels have been studied by Marder and Marder [5] and Maki et al. [6] respectively. It has been shown that the microstructure of lath martensite is characterized by packets and blocks, which are composed of laths, in the original austenite grain as shown in Figure 1.3. Thus a prior austenite grain, during its martensitic transformation, gets partitioned into several packets (marked as A in Figure 1.3). Each packet is further subdivided into blocks (marked as B in Figure 1.3). Packets consist of parallel laths with the same habit plane. Each block is made up of a matrix of martensite laths having

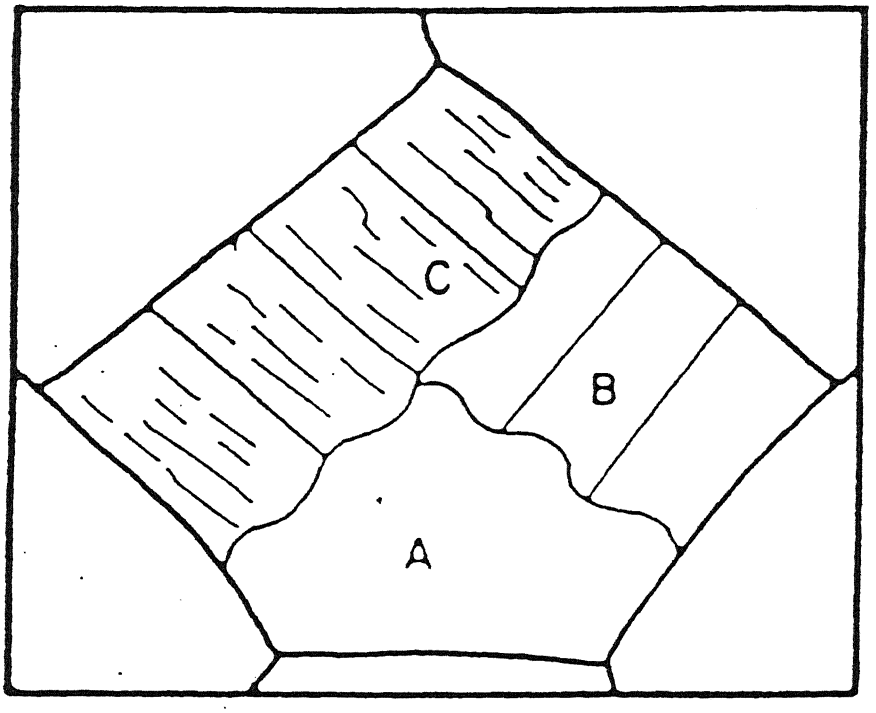

FIG 1.3 Schematic illustration showing the construction of lath martensite structure in a prior austenite grain reported by J. M. Marder and A. R. Marder.[11] Section A represents a packet, section B shows blocks within a packet and section C illustrates an aligned substructure within the block of a packet.

essentially the same variant, namely the identical orientation and the identical habit plane. The blocks are separated from one another by high angle boundaries [5].

Maki et al.[6] have shown that packets and blocks in martensites of 18% maraging steels are clearly defined. Morphological features studied on coarse prior austenite grain size maraging steel samples (grain size varying from 59-445 μm) revealed that blocks were parallel and well defined and were extended almost throughout the packet. These features are in contrast to morphology of lath martensites formed in low carbon (C $\leq$ 0.2 wt%) steels where blocks of martensite do not develop distinctly and are generally wedge shaped and often segmented. A schematic diagram showing morphological features in low carbon and maraging steel martensites is shown in Figure 1.4.

1.3.3 Austenite Reversion

As indicated by the Fe-Ni phase diagram (Figures 1.1 and 1.2), the iron-nickel martensites are metastable and can revert to ferrite or/and austenite. The austenite reversion, i.e., reaction involving $\alpha' \longrightarrow \gamma$ transformation, depending on the chemical composition of the maraging steel and the transformation temperature, can be slow or rapid. The slow transformation involves redistribution of constituent elements, i.e. it is diffusion assisted, and results in a characteristic 'stripe' pattern having austenite layers separated by regions of ferrite [7]. On the other hand, rapid reversion involves martensitic transformation mechanism, i.e. it is diffusionless shear type of transformation.

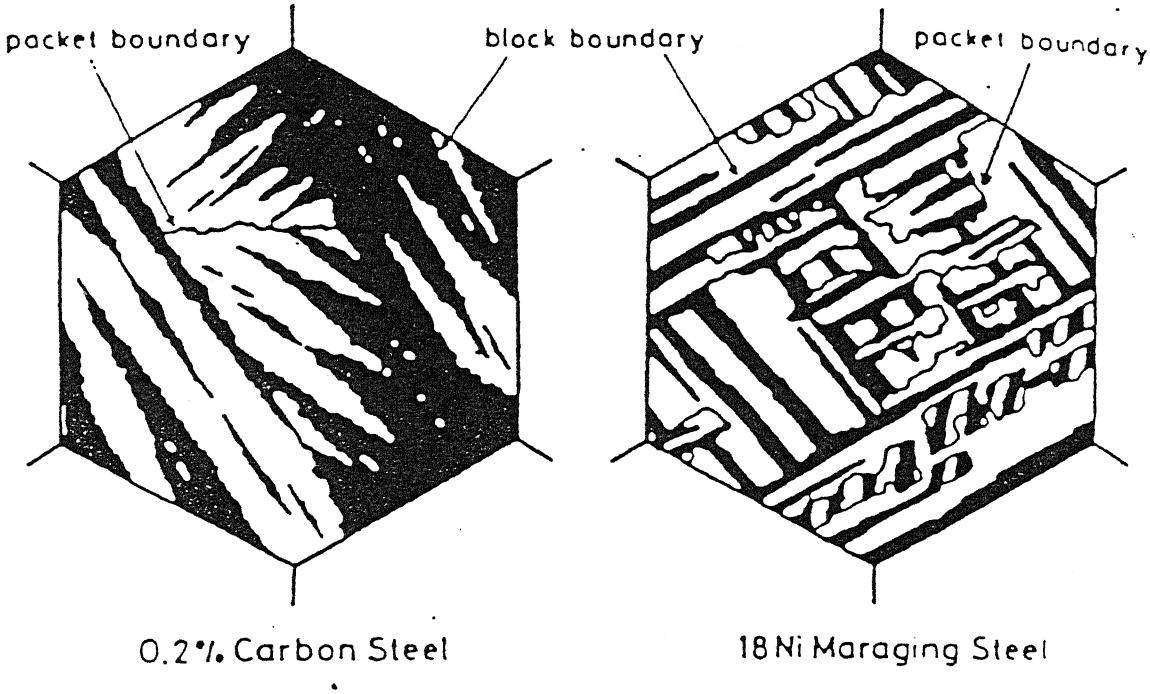

FIG.1.4 Schematic illustrations showing the morphological characteristics of lath martensite structure in 0.2% C steel and 18% Ni maraging steel.

A. Diffusion-Assisted Austenite Reversion

Metastable martensite can decompose by a diffusion controlled reaction to ferrite and austenite after prolonged holding at temperatures below austenite start temperature (A_s). Depending on the temperature and composition the austenite thus formed may become so rich in Ni that its M_s temperature lies below the ambient temperature. As a result retained austenite may often be found in the microstructures of maraging steels. The rate of austenite reversion reaction depends on temperature and, fortunately for maraging steels, this rate at temperatures of the order of 485^{o}(the typical aging temperature) is slow enough so that precipitation hardening can be achieved before the reversion reaction predominates.

The rate of austenite reversion is also quite sensitive to composition. In binary iron-nickel alloys increasing nickel levels generally tends to accelerate austenite formation [3]. In steels containing other alloying elements the effect of individual elements will partly depend on whether the element is an austenite or ferrite stabiliser. A much stronger effect probably results from change in matrix composition that accompanies precipitation. Titanium, for example, has been found to markedly retard reversion, evidently because the formation of Ni_3Ti lowers the nickel content of the matrix [1]. Molybdenum additions, on the other hand enhance reversion [1]. In this case the austenite reversion has been suggested to be associated with the dissolution of Ni_3Mo and the formation of Fe_2Mo presumably, when Ni_3Mo goes into solution causing the local enrichment of the matrix with

nickel favouring the reversion process.

In binary alloys of Fe-Ni the austenite reversion reaction has been suggested [8] to be a one step process while in more complex alloys it has been found to be occurring by two successive steps. Austenite reversion has generally been found to occur at the boundaries of the martensite platelets (packets, blocks or laths).

B. Diffusionless Austenite Reversion

Austenite can also be formed by heating the martensite above the A_s temperature. In this case the transformation from martensite to austenite is by shear and the resultant austenite has the same chemical composition as that of the initial martensite. Crystallographically this transformation is similiar to the austenite to martensite transformation.

Austenite reversion in 18% Ni maraging steels has been studied by Hosomi et al. [9] and Maki et al. [6]. Maki et al. obtained austenite start, A_s, and austenite finish, A_f temperatures of 18% Ni maraging steel containing ~ 9 wt% Co, 5 wt% Mo and 0.7 wt% Ti by resistivity change measurements. A_s and A_f for this steel were found to be 684°C and 786°C respectively.

Microstructural examination of transformed structure in all the cases showed that the location of the reversed austenite grain boundaries exactly corresponded to the prior austenite grain boundaries of the original specimen and hence there was no change in austenite grain size by the $\alpha' \longrightarrow \gamma$ reverse transformation. Retention of the grain size in reverted austenite has also been reported by other workers [10] and has sometimes been referred to

as the microstructural memory effect'. It has been suggested that the propensity for structure inheritance depends on a number of factors namely [11]

i) alloying elements

ii) plastic deformation imparted to the material prior to its transformation

iii) heating rate

iv) volume effect of the $\alpha' \longrightarrow \gamma$ transformation.

Sadovskiy et al. have shown that retained austenite does not have a decisive role in the microstructural memory effect [7]. For example distinct structural inheritance was observed in maraging steels with or without the presence of retained austenite.

Further, it has been observed that the reversed austenite, right after the completion of $\alpha' \longrightarrow \gamma$ transformation is unrecrystallized irrespective of holding temperature. With an increase in holding time or in holding temperature, the reversed austenite changes from the unrecrystallized to the recrystallized austenite . Because of the recrystallization of the reversed austenite, the austenite grain size becomes fine, and then increases with an increase in holding temperature due to the grain growth.

In the case of Fe-30 ~ 34% Ni alloys in which $\alpha' \longrightarrow \gamma$ reverse transformation takes place at fairly low temperatures by the mechanism of shear transformation, the recrystallization of reversed austenite occurs by further heating because of a high density of lattice defects caused by shear mechanism of martensitic reverse transformation [12,13]. In contrast to Fe -30 ~34% Ni alloys, austenite reversion in maraging steels, has

been suggested to be occurring partly by the diffusional process in addition to the shear mechanism because of their high A_s and A_f temperatures. Recrystallization behaviour of reversed austenite in 18% Ni maraging steel has been schematically shown in figure 1.5.

Sadovskiy et al have shown that in 18% Ni maraging steels austenite reversion can occur during heating in three distinct ways [7];

(i) by the appearance of plate like nuclei of austenite of one orientation which merge together during further growth and secure reconstruction of the prior austenite grain.

(ii) by means of nucleation of equiaxed austenite in addition to plate-like austenite.

(iii) by means of oriented formation of infralath nuclei of austenite of several orientations.

These orientations are related to the initial α' by martensite orientation relationships. When phase transformation is complete this kind of nucleation mechanism does not result in the recovery of the prior austenite grain, but in the appearance of a group of fine grains which are in specific orientation relation with the original α' grain. This mechanism therefore does not contradict the general observation of structural inheritance in maraging steels.

1.3.4. Aging Behaviour and Kinetics

After transformation to martensite most maraging steels are aged for 3 to 5 hours in the temperature range of 480°C - 500°C. Two main processes [1] leading to hardening may occur during aging

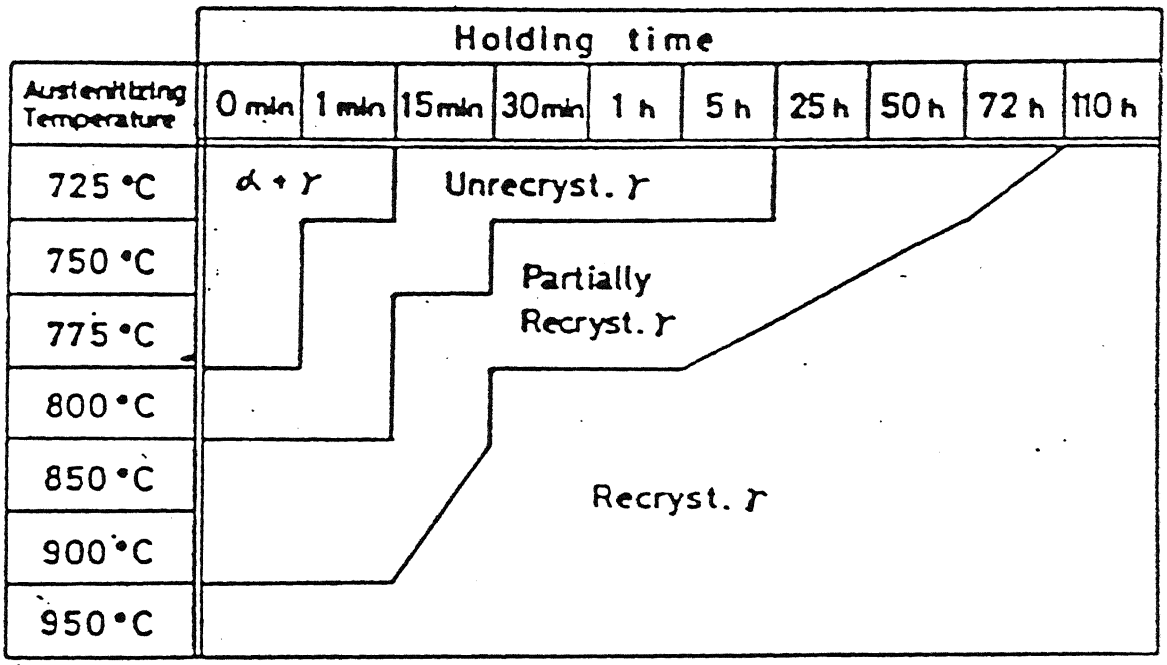

FIG.1.5 Structure change of reversed austenite with holding (austenitizing) temperature and holding time in 18%Ni maraging steel (heating rate: 100°C/min); solution treated specimen.

(a) Precipitation of various intermetallic compounds, sometimes preceded by the formation of thermodynamically metastable intermediate phases.

(b) Ordering in Co-containing solid solution.

Precipitates are formed in various morphologies like needles, ribbons, disks and spheres [14-17]. The most often reported intermetallic is Ni_3Mo. In the intial stages of aging the Ni_3Mo metastable precipitation is favoured because of the low lattice misfit between the precipitate and the matrix. Aging for longer times and/or higher temperature (>480°C) leads to a gradual increase in coherency stresses and the Ni_3Mo is therefore replaced by a more stable Mo-containing precipitate such as Fe_2Mo or σ-phase (Fe-Mo) [1].

The titanium-containing intermetallic most often found to precipitate during aging is μ-Ni_3Ti but the presence of the σ (FeTi) phase has also been reported occassionally. It is possible that some more complex intermetallics such as $Ni_3(MoTi)$ are also formed in the process of aging.

The mechanisms of different precipitation processes are not fully understood. There is some evidence that pre-precipitate zones may form during the initial stages of age hardening. Garwood and Jones [17] have suggested that there is a G.P. zone stage in which segregates are formed parallel to the $[111]_{bcc}$ direction. In Ti containing alloys, Miller and Mitchell [14] suggested that titanium initially forms metastable, ordered bcc zones of Ni_3Ti. These zones are subsequently replaced by η-Ni_3Ti.

The nucleation of the precipitates during aging generally occurs on dislocations and lath boundaries. Because of

the high density and uniformity of dislocations in the lath martensite, the precipitates are homogeneously distributed unless a preferred orientation of dislocation exists. In case of preferred orientation of dislocations, precipitates may also get oriented [14, 17].

Takaki and Tokunaga [18] have investigated the aging reaction using specific heat, hardness and resistivity measurements. Figure 1.6 shows the specific heat versus temperature curves of ternary and quarternary martensitic alloys. A heat evolution occuring around 347°C (620°K) corresponds to formation of an ordered phase. The ordered phase [19] is suggested to be Fe(Ni,Co). The 467°C (740°K) peak evolution is due to the formation of Mo rich zones [20-23] and the absorption around 497°C (770°K) is due to the reversion of these zones.

It has been shown that the critical condition [23]for appearance of 467°C (740°K) evolution peak is given by the following expression

$$\% \text{ Co} \times \% \text{ Mo} = 32 \qquad (1.1)$$

The 527°C (800°K) peak evolution is attributed to formation of Ni_3Mo [15].

Takaki and Tokunaga [18] concluded that age hardening of Ni maraging steels without Ti or Al addition is mainly due to the formation of Mo rich zones prior to the precipitation of Ni_3Mo.

1.4.1. CONVENTIONAL HEAT TREATMENT OF MARAGING STEEL

As mentioned earlier, microstructures of heat-treated maraging steels consist of fine precipitates of intermetallic compounds uniformly distributed in a matrix of Fe-Ni martensite [1]. Such a microstructure is conventionally achieved by a

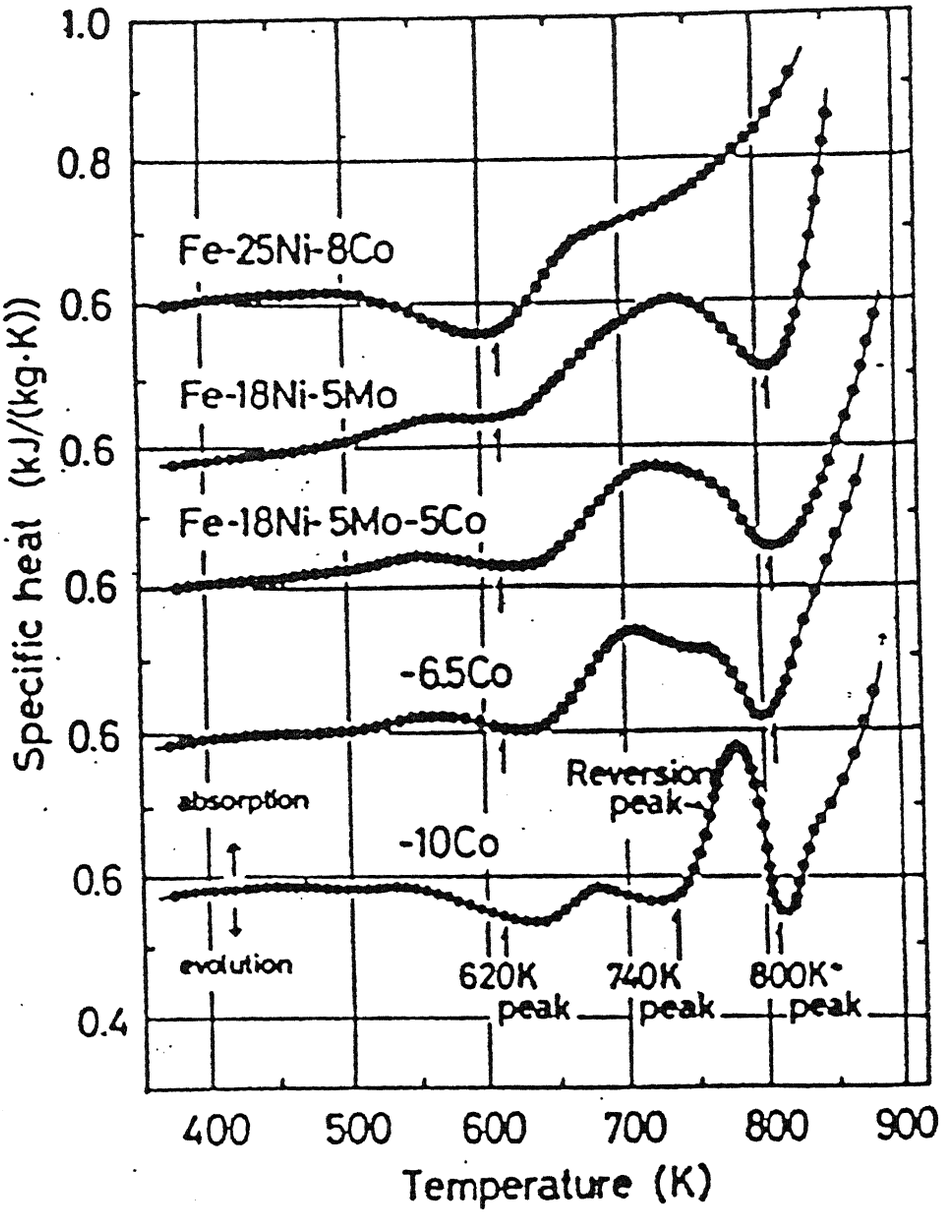

FIG.1-6 Specific heat versus temperature curves of the ternary and quaternary alloys: Heating rate is about 0.025 K/s.

two-stage heat treatment involving

(a) solution treatment in the austenitic phase field followed by martensitic transformation.

(b) Aging of martensite

The commercial heat treatment of these steels consists of solutionising at 820°C for 1 hr per 25 mm section thickness followed by air cooling and then ageing at 480°C for 3 hrs [3].

1.4.2. UNCONVENTIONAL HEAT TREATMENTS OF MARAGING STEELS

The basic microstructural unit controlling the strength and fracture of lath martensites has been suggested to be the packet [24-30] or block [31,32]. Because blocks in 18% Ni maraging steels consist of a set of parallel laths with essentially the same variant and are separated from one another by high angle boundaries [5] it should be considered that the block in maraging steel is the basic structural unit of lath martensite structure to act as a barrier to deformation and fracture.

Maki et al have studied the relationship between prior austenite grain size and packet size and block width [6]. Variation of packet size and block width and the ratio of grain size to packet size (G.S./P.S.) with prior austenite grain size has been shown in Figures 1.7 and 1.8 respectively. It can be seen that both packet size and block width as well as G.S./P.S. decrease by decreasing the prior austenite grain size.

It is not surprising, therefore, that efforts are made to develop alternative heat treatments for maraging steels from the point of view of refinement of prior austenite grains. Specifically, $\alpha' \rightarrow \gamma$ cyclic transformation and several thermomechanical treatments such as cold rolling before solution

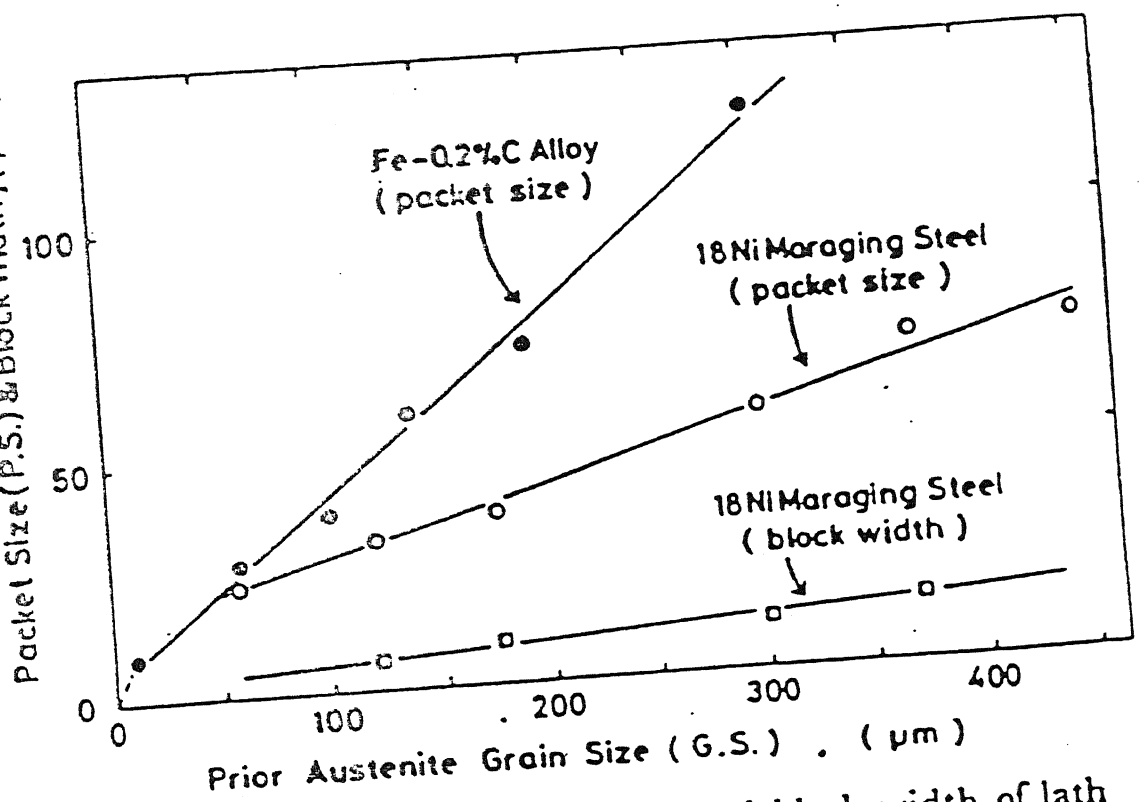

FIG.1·7 Change in the packet size and block width of lath martensite with the prior austenite grain size in Fe–0.2%C alloy and 18%Ni maraging steel.

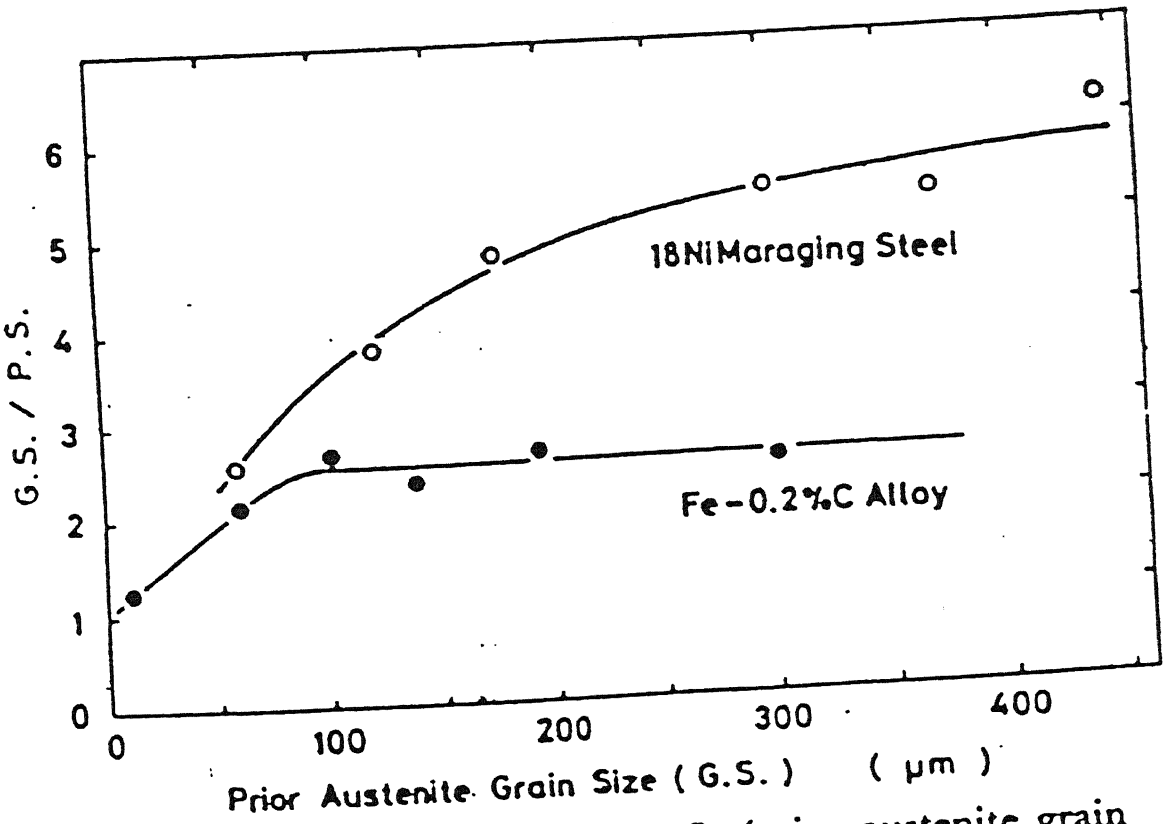

FIG.1-8 Change in the ratio of G.S. (prior austenite grain size) to P.S. (packet size of lath martensite) with the prior austenite grain size in Fe–0.2%C alloy and 18%Ni maraging steel.

treatment and hot rolling during cooling from the solution temperature [33] have been attempted. Further, since the nature of the precipitation of intermetallic compounds and their aging kinetics are likely to be affected by the distribution of alloying elements within the martensitic structure, the effect of solution treatment temperature and cooling rates have also been subjected to re-examination. For example, Muneki et al. have observed that by solutionizing at conventional temperature, i.e. 820^{o}C, a part of Mo remains as the retained precipitate, which reduces the ductility and toughness leading to the easy occurrence of unstable fracture at a low stress level [34]. It was suggested, therefore, to perform the solutionizing at higher temperature. A new heat treatment schedule [2] has been suggested according to which the solutionising is carried out in two stages. It consists of annealing at 930 ± 10^{o}C for 80 minutes, air cooling and re-annealing at 760 ± 10^{o}C for 80 minutes followed by air cooling. It is then aged at 480^{o}C for 3 hrs. Some investigators [2] have reported a better combination of strength and toughness, if a double annealing treatment is employed prior to ageing. However, metallurgical reasons for the enhancement of properties by the double annealing treatment have not been clearly given.

1.5 DYNAMIC STRAIN AGING OF 18 Ni MARAGING STEELS :

It has been generally accepted that the hardening of Ni maraging steels at the conventional aging temperature (conventional aging temperature is 480^{o}C) is due to the precipitation of the intermetallic compound involving Mo on dislocations introduced by the martensitic transformation [18]. However, it is probable that the nature of aging kinetics is

complex prior to the precipitation of the intermetallic compound [18]. For example, Peters and Cupp [20] have suggested that at aging temperatures below 457°C, Mo rich zones, [20-23] named "matrix precipitates", are formed in the matrix away from dislocations. But Takaki and Tokunaga [18] suggested that Mo rich zones are formed within the stress field of dislocations by "a kind of strain aging".

Hayes [35] examined the aging kinetics of the 18 Ni 250 maraging steel under dynamic aging conditions. Hayes [35] studied the dynamic aging of 18 Ni 250 maraging steel by conducting a series of uniaxial tensile test on single solutionized samples. The test temperatures were varied from 204 to 454°C and the strain rate from 1.16×10^{-4} to 1.5×10^{-2} s^{-1}.

1.5.1 Phenomenology

In a tensile [36] test, the specimen (suitably gripped between two cross heads, one moving and the other fixed) is deformed at a constant nominal strain rate determined by the velocity of the moving cross head. At any instant of time, the total strain ε, the plastic strain ε_p in the specimen, and the elastic strain ε_e of the specimen machine system are related by

$$\varepsilon = \varepsilon_p + \varepsilon_e \qquad (1.2)$$

$$\dot{\varepsilon} = \dot{\varepsilon}_p + \dot{\varepsilon}_e \qquad (1.3)$$

$$= \dot{\varepsilon}_p + \frac{\dot{\sigma}}{E_s} \qquad (1.4)$$

where $\dot{\sigma}$ is the stress rate, E_s is the elastic modulus of the specimen-machine system, $\dot{\varepsilon}$ is the imposed strain rate and $\dot{\varepsilon}_p$ is the plastic strain rate.

The condition for load drop/serrations is that the plastic

strain rate $\dot{\varepsilon}_p$ exceeds the imposed strain rate $\dot{\varepsilon}$, i.e., whenever there is a sudden increase in $\dot{\varepsilon}_p$ a load drop occurs.

1.5.2 Physical processes that cause serrated flow :

(i) *Ordering* : In alloys undergoing order-disorder [36] transformation, gradients or modulations in order encountered by moving dislocations can lead to serrated flow. In case of short range order stress will increase by an amount, $\Delta\sigma$ given by [37]

$$\Delta\sigma = \gamma/b \qquad (1.5)$$

where γ is the increase in the surface energy of slip plane, since a dislocation of burgers vector b in its passage will lower the order of the lattices. If in an avalanche of dislocations this order is destroyed rapidly, a drop in flow stress will result.

This theory was later extended by Schoeck and Seeger [38]. The basic concept of "Schoeck ordering" is that if an ordered arrangement of atoms causes distortion in the lattice, the formation of an ordered region around dislocations will be favoured in those positions where the lattice strain due to ordering complies with the local stress tensor of the dislocation i.e. where elastic strain energy in the crystal is reduced by ordering. In other words, the line energy of the dislocation is lesser by a certain amound compared with a dislocation surrounded by a random or disordered distribution of solutes. In order to move the dislocation we have to apply a certain force since we must supply energy to bring the dislocation into a region where there is random distribution of solutes. Since for the process of ordering, only atomic interchanges between neighbouring lattice sites are necessary and no long range diffusion of atoms is involved, it takes place in a relatively short time and is not

influenced by the concentration of vacancies in the material.

Low value of activation energy in CuAu [39] has been attributed to enhanced migration of atoms in a narrow region (a few burgers vector wide) near the core of the dislocation.

(ii) *Twinning :* Another phenomenon that can cause serrations is continued mechanical twinning as has been reported for an Fe-25 at% Be alloy [36].

(iii) A sudden increase in the specimen temperature due to adiabatic heating is another possibility. This has been found to occur in tests at cryogenic temperatures [36].

(iv) Phase transformations induced by stress and strain can also cause serrated flow [36].

CHAPTER - 2

AIM OF THE PRESENT WORK:

Static strain aging behaviour of 18 Ni 250 maraging steel will be examined in the present study. Two types of solutionising treatments will be carried out namely single solutionising and double solutionising and then a comparison of mechanical properties produced by the two treatments will be done. Also it is intended to study the effect of heat treatment on the microstructural features of 18 Ni 250 maraging steel.

CHAPTER - 3

EXPERIMENTAL PROCEDURE

3.1 MATERIAL

Commercial grade of maraging 250 steel in the form of sheets was obtained from Mishra Dhatu Nigam Ltd, Hyderabad. The material was manufactured by double vacuum melting followed by ingot making, rough forging, hot rolling and cold rolling. The thickness of the sheet being 4.8 mm.

The chemical composition of the material supplied is shown in Table 3.1.

3.2 THERMOMECHANICAL TREATMENT

Samples of approximately 65 mm x 40 mm x 4.8 mm were cut from the sheets. These samples were homogenized at 1060°C for 60 minutes in a horizontal muffle furnace. The homogenizing furnace, made of Inconel tube, had the capability of providing controlled atmosphere. Homogenizing treatment of all the samples was done under argon atmosphere.

Homogenized and preheated samples were subsequently hot rolled on a 2-high rolling mill having 135 mm diameter rolls rotating at a speed of 55 rpm. A total of 80.4 % thickness reduction was given in 9 passes. Details of the thermomechanical working schedule are shown in Table 3.2. A schematic diagram of the rolling schedule is shown in Figure 3.1. All the hot rolled scheets were immediately water quenched (within 5 s) after the final pass.

TABLE 3.1

Maraging Steel type	Nominal Composition Ni	Co	Mo	Al	Ti	Cr	C (Max)	Fe
18 Ni 250	18	8	4.8	.1	.4	-	.03	68.7

TABLE 3.2

Rolling Schedule

Specimen Thickness (mm)		Rolling Temperature (°C)	No. of Passes	Total Reduction (%)
Initial	Final			
4.80	3.15	1060	3	34.3
3.15	1.80	1000	3	42.8
1.80	0.94	960	3	47.7

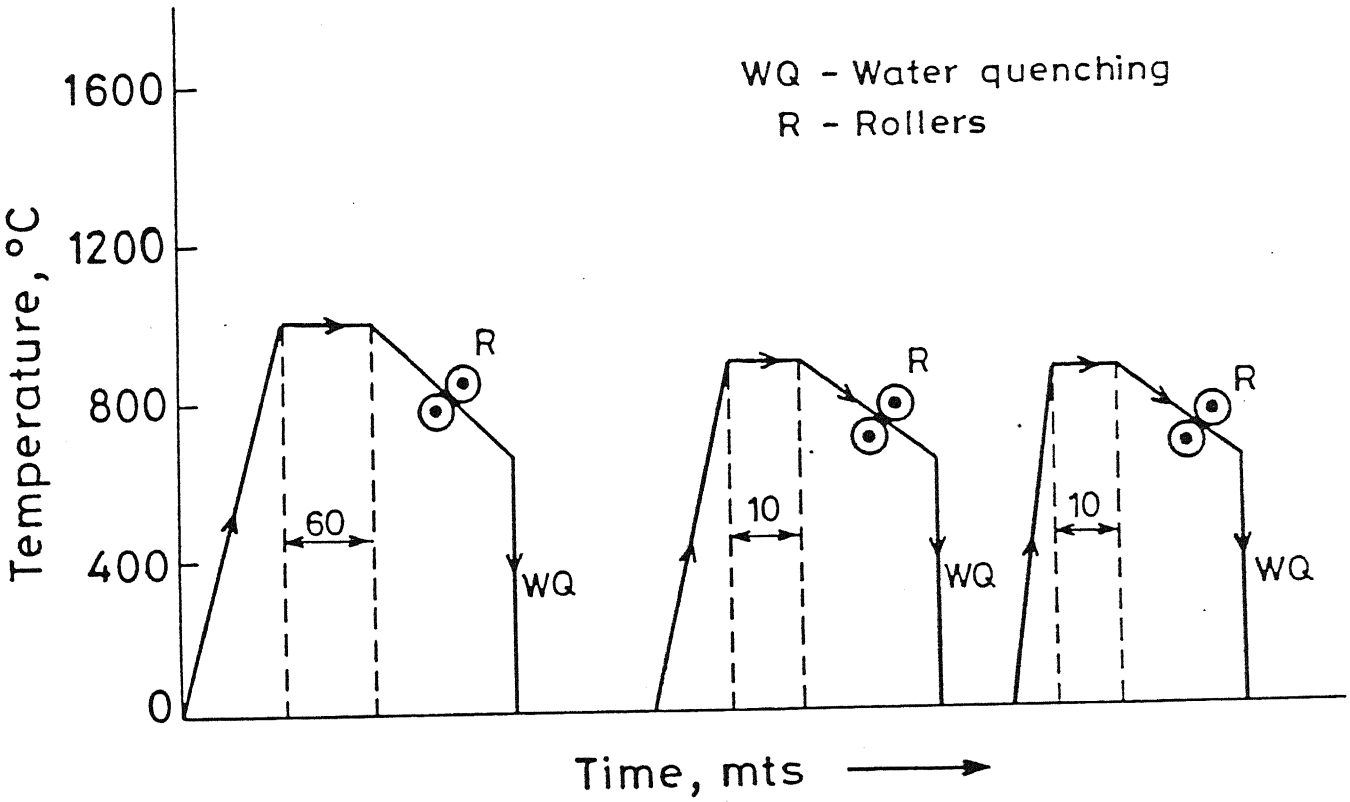

Fig. 3.1 Temperature - time diagram showing thermomechanical treatment.

3.3 HEAT TREATMENT

Sheet samples of maraging 250 steel were subjected to thermomechanical treatment discussed in Section 3.2. Tensile test samples from this material were made in the workshop. Tensile test samples as well as samples for microstructural examination were subjected to single and double solution treatments.

A. Single Solution Treatment:

Holding of samples at a temperature of 935°C for 35 minutes followed by quenching in agitated water.

B. Double Solution Treatment:

(i) Holding of samples at a temperature of 935°C for 35 minutes followed by quenching in agitated water.

(ii) Holding of samples at a temperature of 760°C for 45 minutes followed by quenching in agitated water.

3.4 AGING TREATMENT

The single as well as double solutionised samples were aged in a muffle furnace. Three aging temperatures of 400°C, 450°C and 480°C were chosen. Samples were aged upto 4 hrs. starting from 1 hr. and stopping after each 0.5 hr. Table 3.3(a) and 3.3(b) show the plan of aging treatment.

3.5 STATIC STRAIN AGING TESTS

3.5.1 The Tensile Test

The aged samples were subjected to a series of uniaxial tensile tests at room temperature.

Tensile specimens were machined and polished on lathe

TABLE 3.3(a)

Aging Schedule

S.No.	Type of Solutionsing	Aging Temperature (°C)	Aging Time (h)
1.	Single Solutionising	400	1.0
2.			1.5
3.			2.0
4.			2.5
5.			3.0
6.			3.5
7.			4.0
8.		450	1.0
9.			1.5
10.			2.0
11.			2.5
12.			3.0
13.			3.5
14.			4.0
15.		480	1.0
16.			1.5
17.			2.0
18.			2.5
19.			3.0
20.			3.5
21.			4.0

TABLE 3.3(b)

Aging Schedule

S.No.	Type of Solutionsing	Aging Temperature (°C)	Aging Time (h)
1.	Double Solutionising	400	1.0
2.			1.5
3.			2.0
4.			2.5
5.			3.0
6.			3.5
7.			4.0
8.		450	1.0
9.			1.5
10.			2.0
11.			2.5
12.			3.0
13.			3.5
14.			4.0
15.		480	1.0
16.			1.5
17.			2.0
18.			2.5
19.			3.0
20.			3.5
21.			4.0

centres. Figure 3.3 shows the standard dimensions of the tensile test specimen. The test pieces were flat.

Testing was performed on an Instron testing machine. All testing was performed in air. All load strain curves were recorded to rupture. A total of 42 load elongation curved were obtained. Each curve corresponds to a particular combination of solution treatment, aging temperature and time. These curves were subsequently analysed. A typical load elongation curve is shown in Figure 3.4.

3.5.2 Analysis of load elongation curves

Prior to tensile test each test sample was measured in thickness and scratch marks were made to measure the gauge lengths. Ultimate tensile strength was measured for each sample by dividing the maximum load on the load elongation curve by the sample cross section area. 0.2% yield strength was also measured from the load elongation curve.

Gauge lengths before and after fracture were measured by travelling microscope % elongation was measured for each sample using the standard formula.

$$\% \text{ elongation} = \left(\frac{L_f - L_o}{L_o} \right) \times 100$$

where L_f = gauge length after fracture

L_o = gauge length before fracture

Vickers Hardness of the samples was also measured.

3.6 MICROSCOPY

In order to study the structural changes associated with thermomechanically treated, solutionised and aged samples,

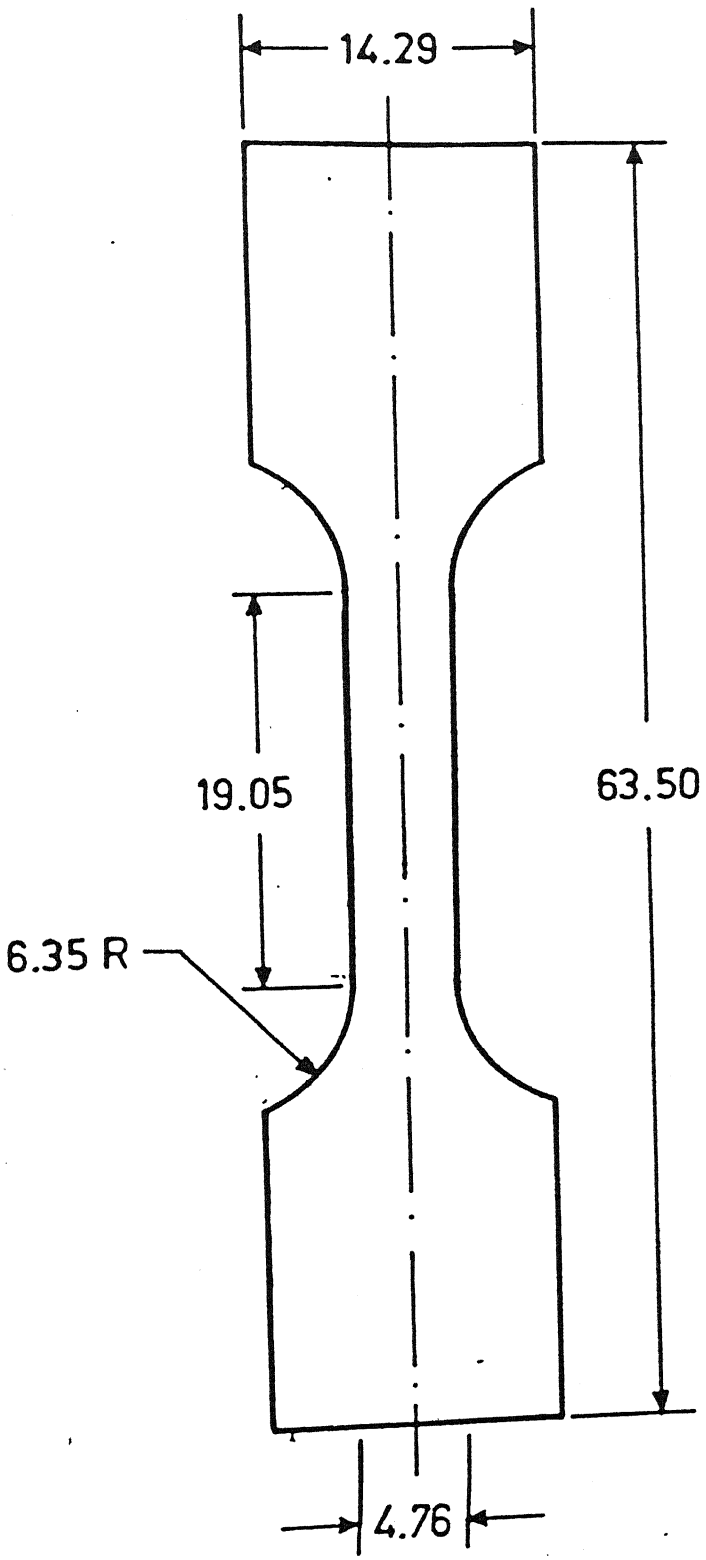

Fig.3.3 Tensile test specimen (units in mm)

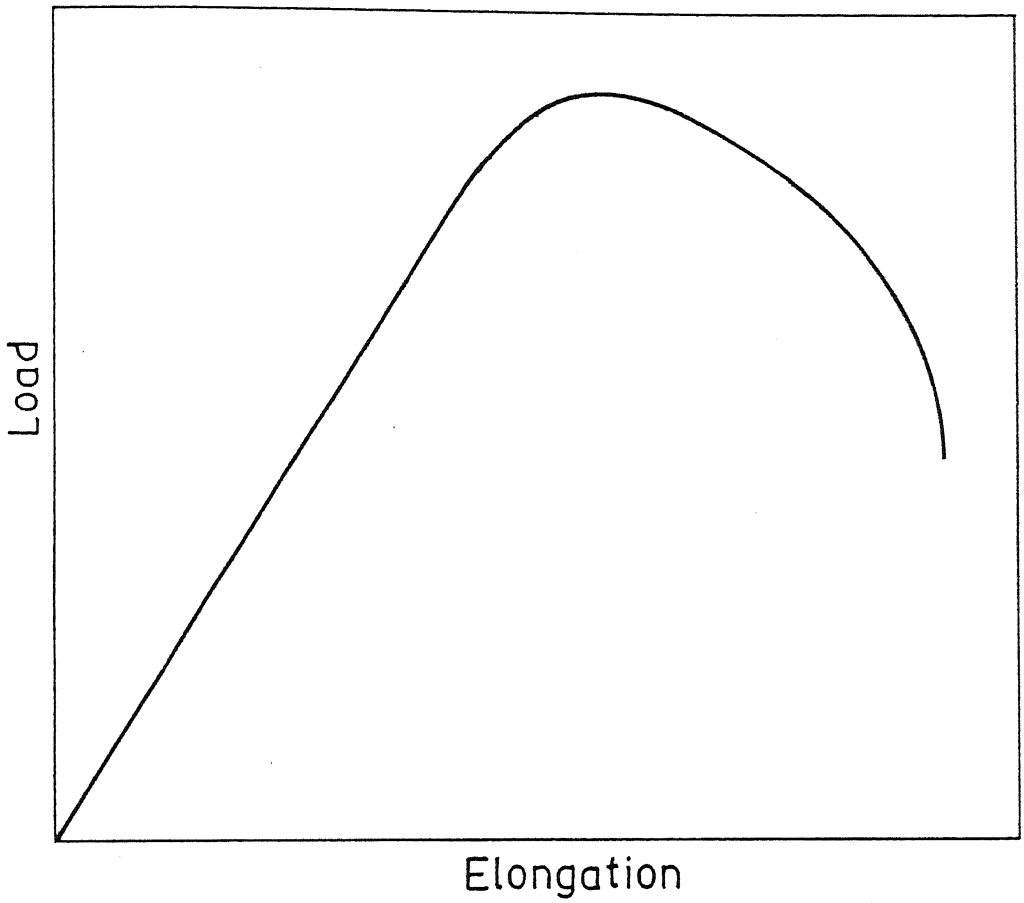

Fig. 3.4. Schematic Plot of Load vs. Elongation.

specimens were prepared for their microstructural examination by optical microscopy and scanning electron microscopy (SEM). Experimental procedure adopted for these purposes are described below.

3.6.1 Optical Microscopy

Metallography samples from thermomechanically treated, solutionised and aged samples were mechanically polished by standard methods to achieve optimum polished surface. The 18% Ni 250 maraging steel is known to exhibit a typical Lath martensite. However the etching is generally difficult to clearly reveal the martensitic structure especially the packet boundaries. Etching the Lath martensite structure of steels used in the present study, therefore, required considerable amount of experimentation. Etching reagents which were tried have been shown in Table 3.4 but results obtained were not found to be satisfactory.

The samples were electrolytically etched in a 10% chromic acid (Cr_2O_3) solution. The experimental set up is shown in Figure 3.2. The polished specimen,S, serves as the anode and C is the steel cathode. The temperature of the electrolyte was maintained at room temperature and voltage was maintained at 6 volts. The etched specimens were seen in optical microscope.

3.6.2 Scanning Electron Microscopy

Metallography samples which were thermomechanically treated and heat treated samples were mechanically polished by standard methods to achieve optimum polished surface. The specimens were etched chemically or electrolytically. The etched specimens were seen in the scanning electron microscope at 15 KV.

TABLE 3.4

Various Etchants and Their Chemical Composition Used for Metallographic Studies in 18% Ni Maraging Steel

Etch No.	Name of Etchant	Reagents
	(a) For Matrix Structure (MS) and Grain Boundaries (GB)	
1.	Modified Ferric Chloride	$FeCl_3$ (0.5 g) + HNO_3 (10 ml) + HCl (20 ml) + dist. water (20 ml)
2.	Acetic Acid-Glycerol	Acetic acid (10%) + HNO_3 (10 ml) + HCl (15 ml) + Glycerine (65 ml)
3.	Vilella's reagent	Picric acid (1 g) + HCl (5 ml) + methanol (95%)
4.	Chromic Acid	Chromic acid 10% - electrolytic etching, 6V
	(b) For Phases	
5.	Ferric Chloride	$FeCl_3$ (5 g) + HCl (10 ml) dist. water to make up 100 ml
6.	Picral	Picric acid (4 g) + HCl (2 ml) HNO_3 (2 ml) dist.water (100ml)
7.	3% Nital	HNO_3 (3%) in methanol
8.	1% Nital	HNO_3 (1%) in methanol
9.	Marble's reagent	$CuSO_4$ (10g) + HCl (50 ml) + dist. water (50 ml)

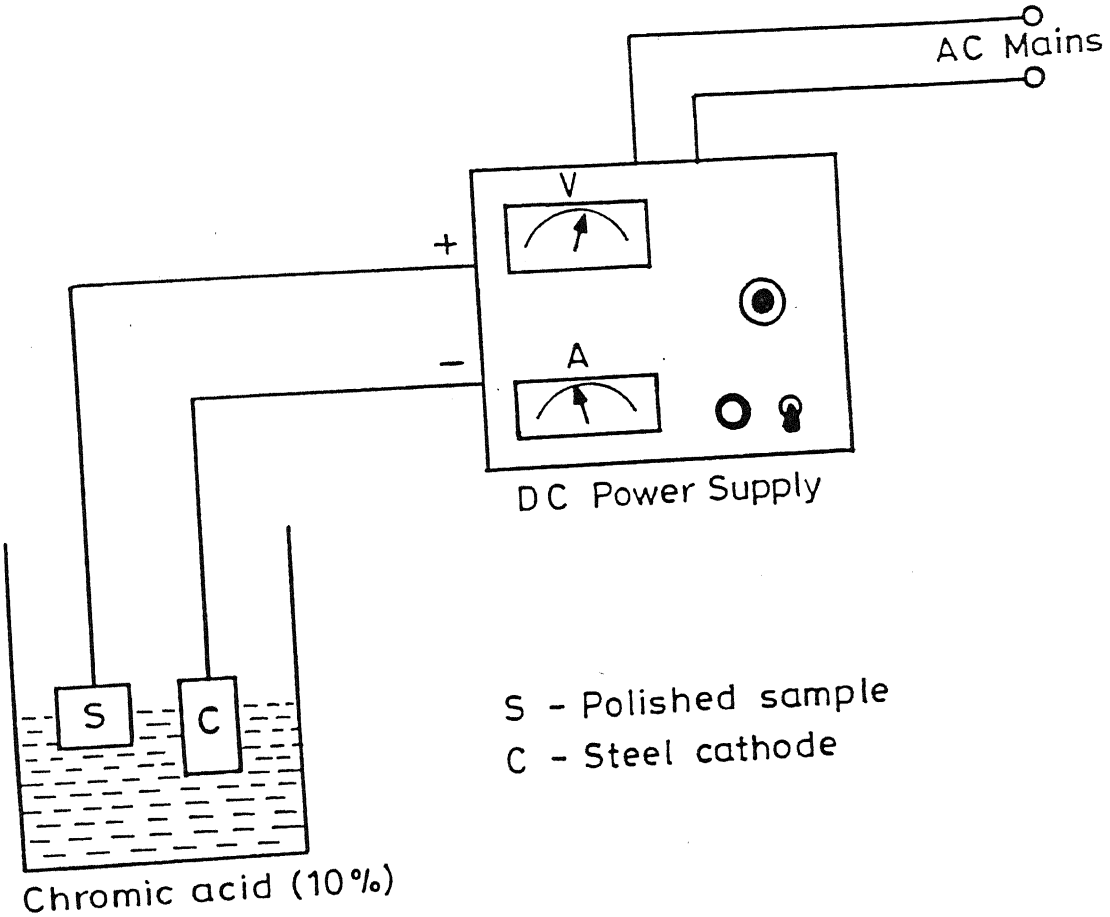

Fig. 3.2 Electrolytic etching apparatus.

CHAPTER 4

RESULTS AND DISCUSSION

4.1 EFFECT OF AGING TIME ON 0.2% YIELD STRENGTH

From figures 4.1 and 4.2 the effect of aging time on 0.2% yield strength with single and double solutionising treatments respectively can be seen. It is observed that at 400°C the 0.2% yield strength keeps on increasing at a comparatively slow rate with aging time. The maximum value attained is 1689 MPa in 4 hrs for single solutionising and 1671 MPa also in 4 hrs for double solutionising. At 450°C the 0.2% yield strength increases at a slightly faster rate with aging time, it attains a maximum value of 1627 MPa in 3 hrs for single solutionising and 1650 MPa for double solutionising also in 3 hrs and then it stabilizes at these values. At 480°C the 0.2% yield strength increases rapidly with aging time and attains a maximum value of 1622 MPa in 2 hrs for single solutionising and 1580 MPa in 2 hrs for double solutionising and then it is expected to go down slowly.

4.2 EFFECT OF AGING TIME ON DUCTILITY

Figure 4.3 shows the variation of elongation percent with aging time with single and double solutionising treatments. It is seen that as aging time increases the elongation percent first goes down and then it increases. The general trend of the curves do not change with different solutionising treatments. At 400°C the lowest elongation percent value is 4.9% for double solutionising and 5.2% for single solutionising, both values attained in 2 hrs. At 450°C the lowest elongation percent value

is 4.6% for double solutionising and 4.8% for single solutionising both values attained in 2.25 hrs. At 480°C the lowest value of elongation percent is 4.4% attained in 2.5 hrs for double solutionising and 4.5% attained in 3 hrs for single solutionising.

4.3 EFFECT OF AGING TIME ON HARDNESS

From figures 4.4 and 4.5 the effect of aging time on hardness with single solutionising and double solutionising treatments respectively can be seen. The nature of the curves is similar to those obtained for 0.2% yield strength vs aging time. At 400°C the maximum hardness is 575 HV attained in 4 hrs for single solutionising and 563 attained in 4 hrs for double solutionising. At 450°C the maximum hardness is 550 HV attained in 3.5 hrs both for single solutionising as well as for double solutionising. At 480°C the maximum hardness reached is 555 HV in 2 hrs for single solutionising and 542 HV in 2.5 hrs for double solutionising.

4.4 COMPARISON OF THE 0.2% YIELD STRENGTH VALUES OBTAINED BY SINGLE SOLUTIONISING AND DOUBLE SOLUTIONISING.

The comparison can be seen by figures 4.6, 4.7 and 4.8. It is observed that at 480°C and 450°C the kinetics of aging are too high to detect any difference between single solutionised and double solutionised steels. But at lower temperatures i.e. 400°C it is seen that the single solutionised steel age hardened at a slightly faster rate than the double solutionised steel. The difference could be seen because kinetics of precipitation hardening is low at lower temperatures.

4.5 COMPARISON OF THE ELONGATION PERCENT AND HARDNESS VALUES OBTAINED BY SINGLE SOLUTIONISING AND DOUBLE SOLUTIONISING.

From figures 4.3, 4.4 and 4.5 we can see that, as above, the effect of solutionising treatments becomes prominent at lower temperature only i.e. we see significant difference only at 400°C and not at 450°C and 480°C.

4.6 MICROSCOPY

4.6.1 Microstructures

Typical lath martensite structure characteristic of maraging steels is seen in all the microstructures, figures 4.9 and 4.10 show it clearly at high magnifications, for the as received (AR) sample. From figures 4.11 and 4.12 which are as received + thermomechanically treated + single solutionised (AR+TMT+SS) and as received + thermomechanically treated + double solutionised (AR+TMT+DS) it is observed that double solutionising gives a coarse structure. If a comparison is made of the microstructures obtained of as received (AR) and as received + thermomechanically treated (AR+TMT) it is seen that at low magnifications no difference is observed (figures 4.13 and 4.14) but at high magnifications it can be seen that the lath width has refined by thermomechanical treatment (figures 4.15 and 4.16). No appreciable difference in structure is observed in figures 4.17, 4.18 and 4.19 which are as received + thermomechanically treated + double solutionised + aged at 400°C for 3 hrs (AR+TMT+DS+400, 3hrs), as received + thermomechanically treated + double solutionsed + aged at 450°C for 3 hrs (AR+TMT+DS+450, 3hrs) and as

received + thermomechanically treated + double solutionised + aged at 480°C for 3 hrs (AR + TMT + DS + 480, 3 hrs) respectively.

4.6.2 Fractography

Inter crystalline brittle fracture is seen in all the fractographs taken which are as follows as received + thermomechanically treated (AR+TMT) figure 4.20, as received + thermomechanically treated + double solutionised (AR + TMT + DS) figure 4.21, as received + thermomechanically treated + single solutionised (AR+TMT+SS) figure 4.22 and as received + thermo-mechanically treated + double solutionised + aged at 480°C for 3 hrs (AR+TMT+DS+480, 3hrs) figure 4.23.

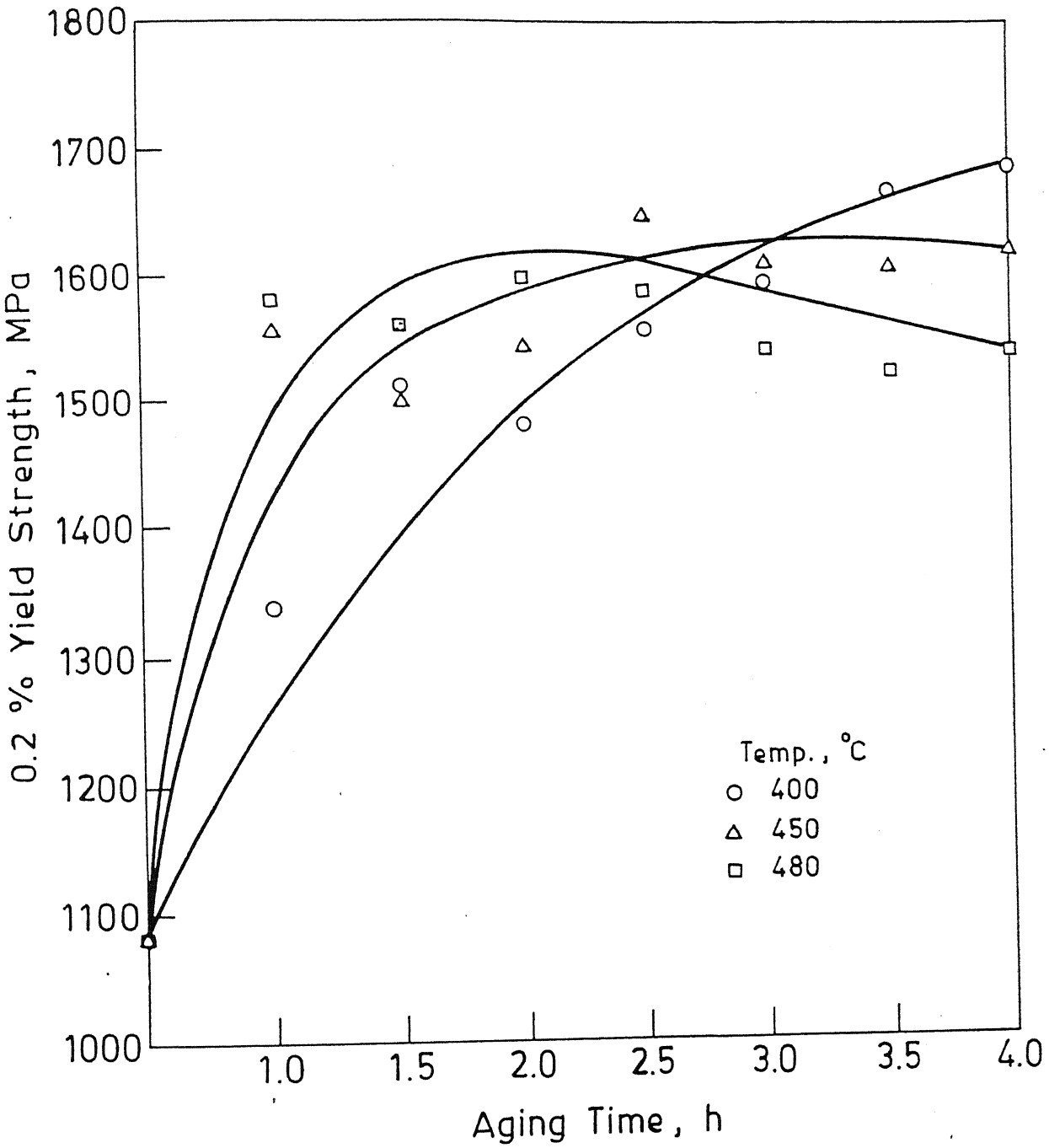

Fig. 4.1. Effect of Aging Time on 0.2 % Yield Strength with Single Solutionising Treatment.

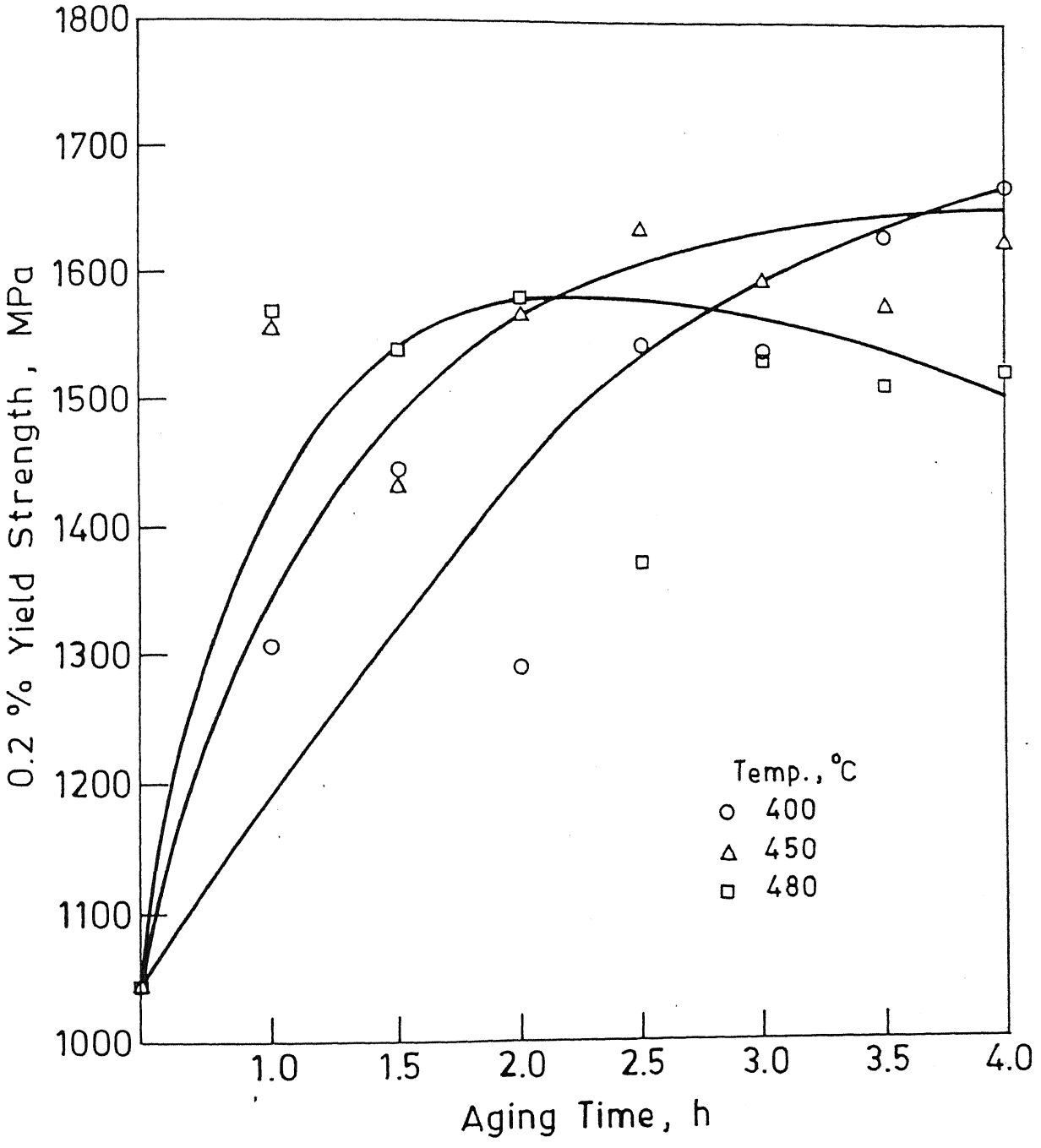

Fig. 4.2. Effect of Aging Time on 0.2 % Yield Strength with Double Solutionising Treatment.

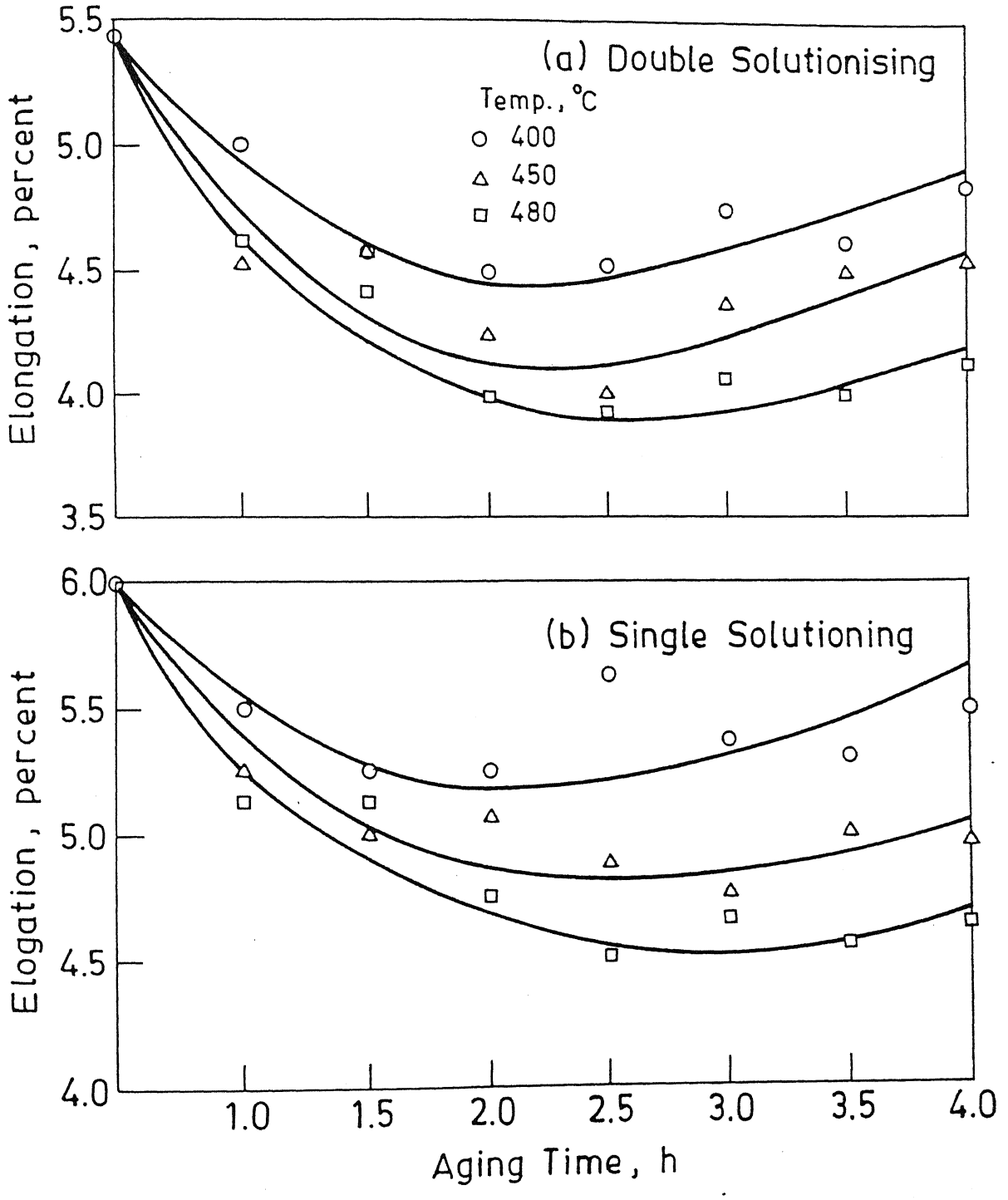

Fig. 4.3. Effect of Aging Time on Elongation Percent with Different Solutionising Treatment.

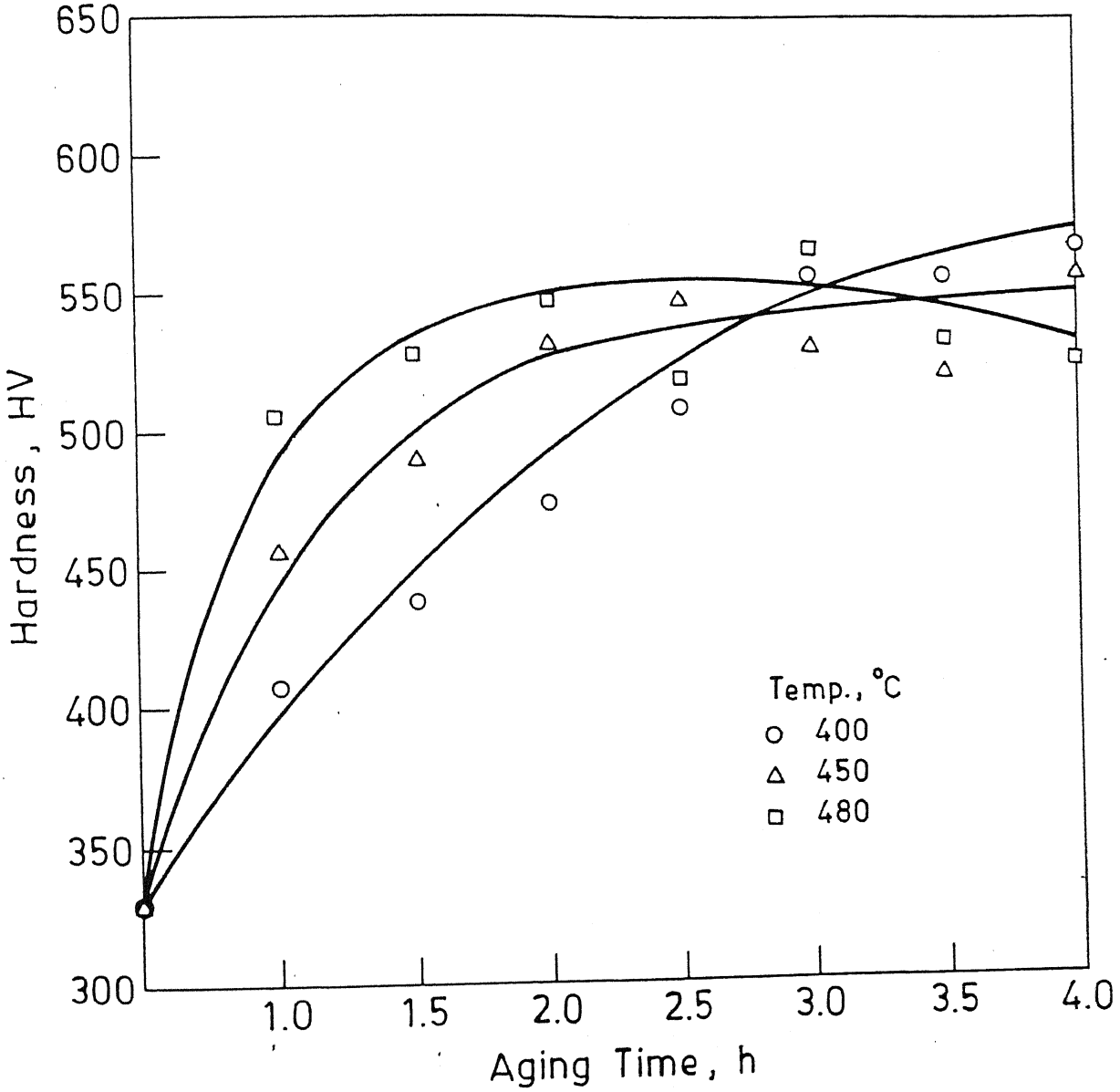

Fig. 4.4. Effect of Aging Time on Hardness with Single Solutionising Treatment.

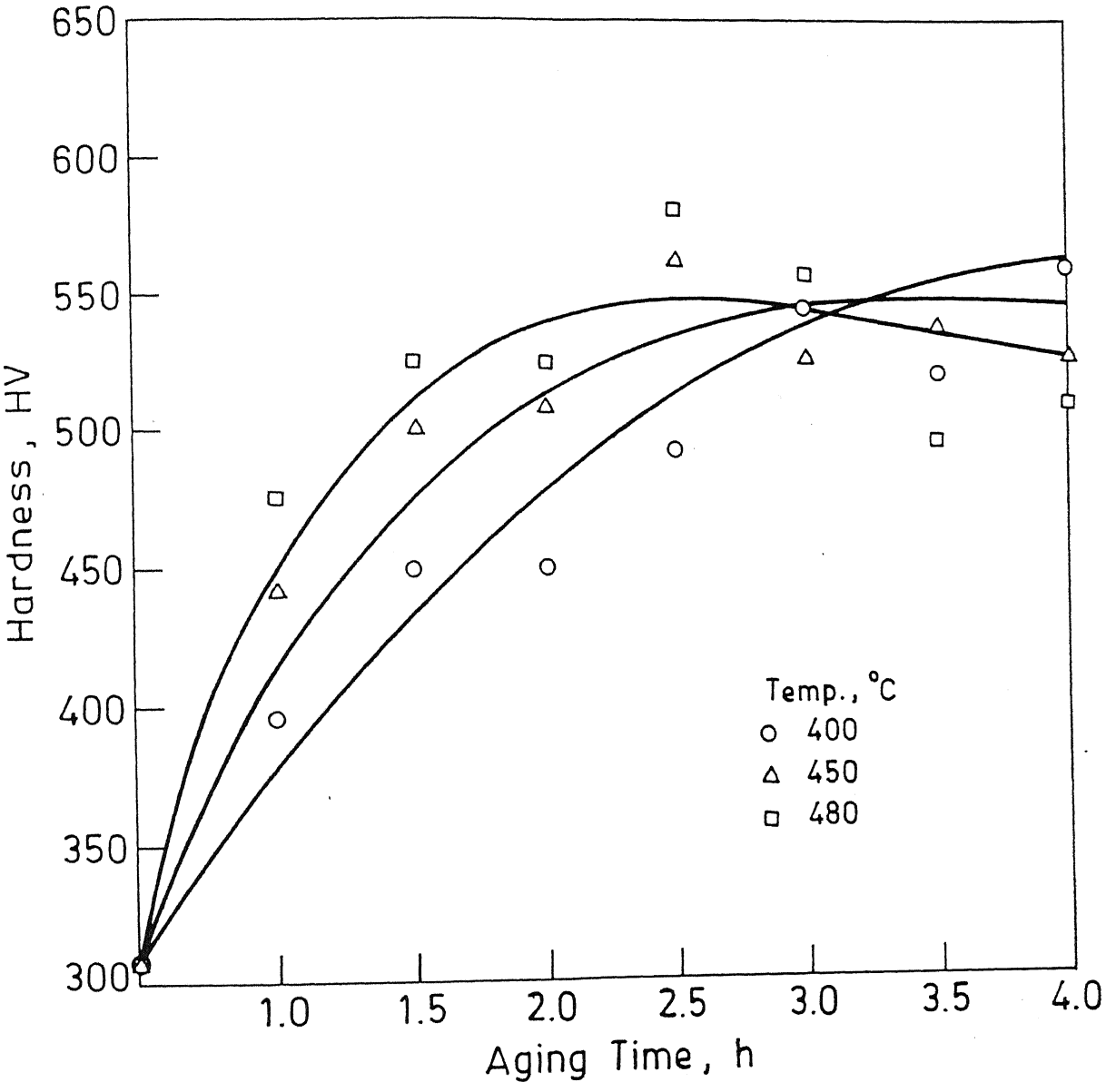

Fig. 4.5. Effect of Aging Time on Hardness with Double Solutionising Treatment.

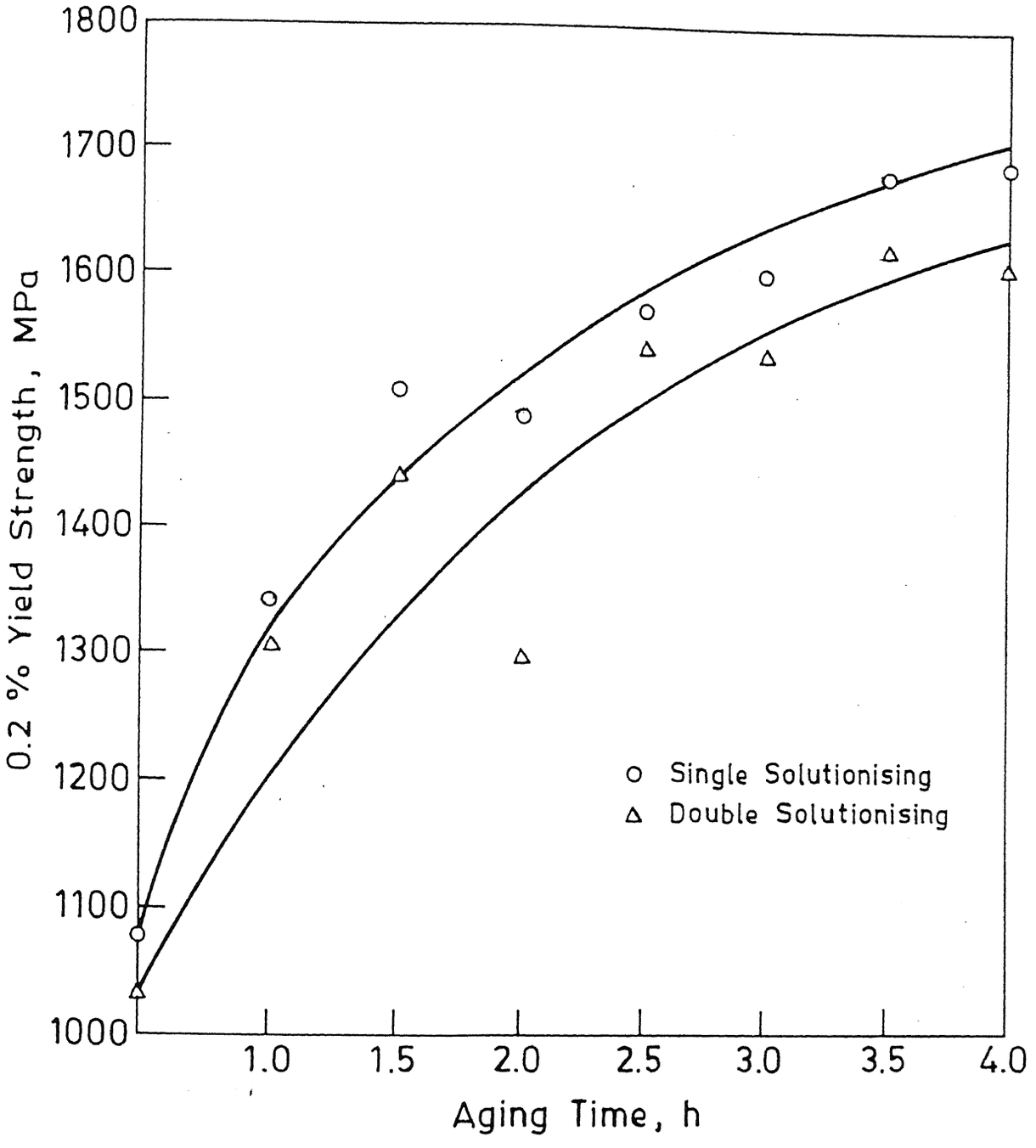

Fig. 4.6. Comparison of the Two Solutionising Treatments at 400 °C.

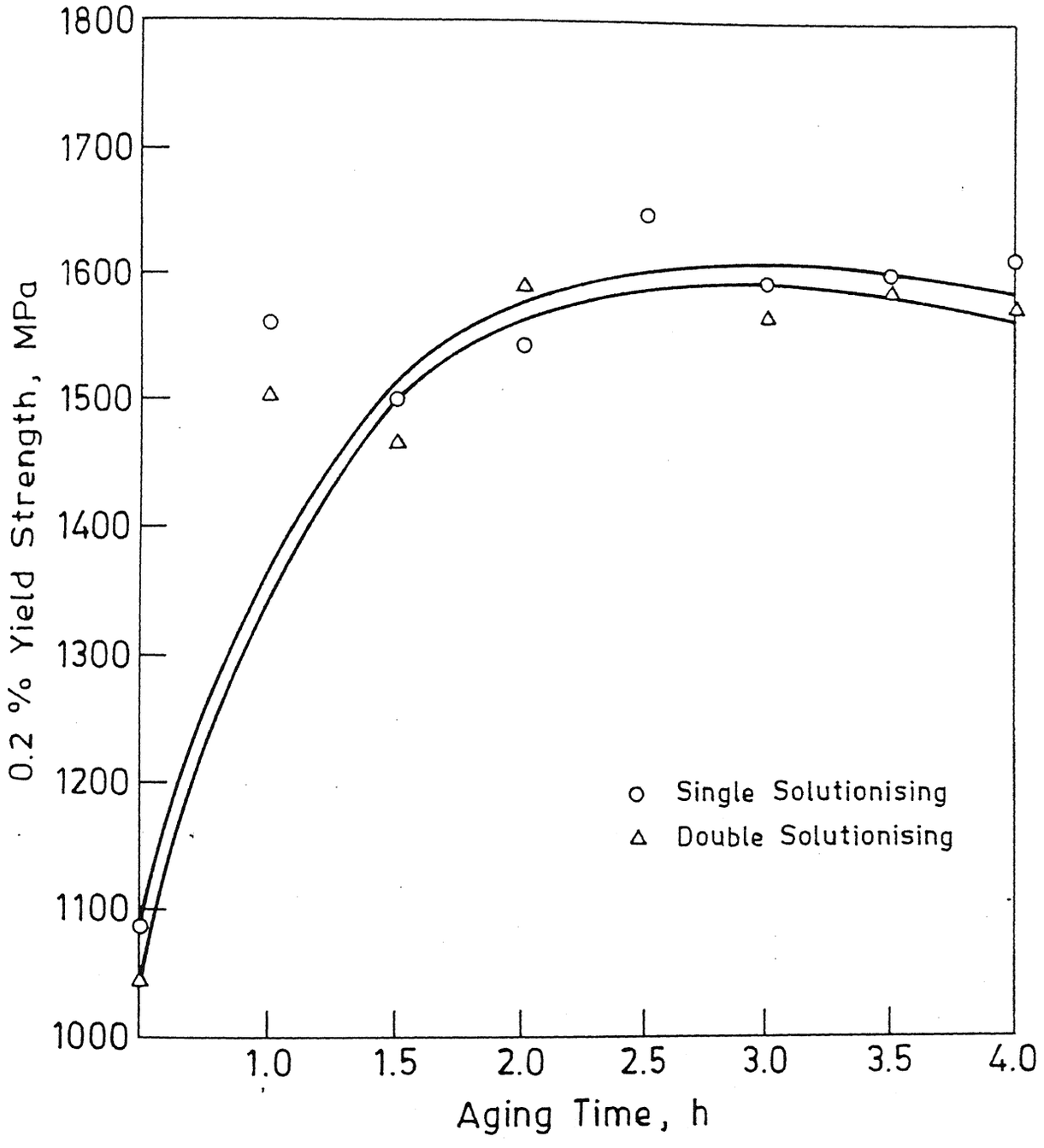

Fig. 4.7. Comparison of the Two Solutionising Treatments at 450 °C.

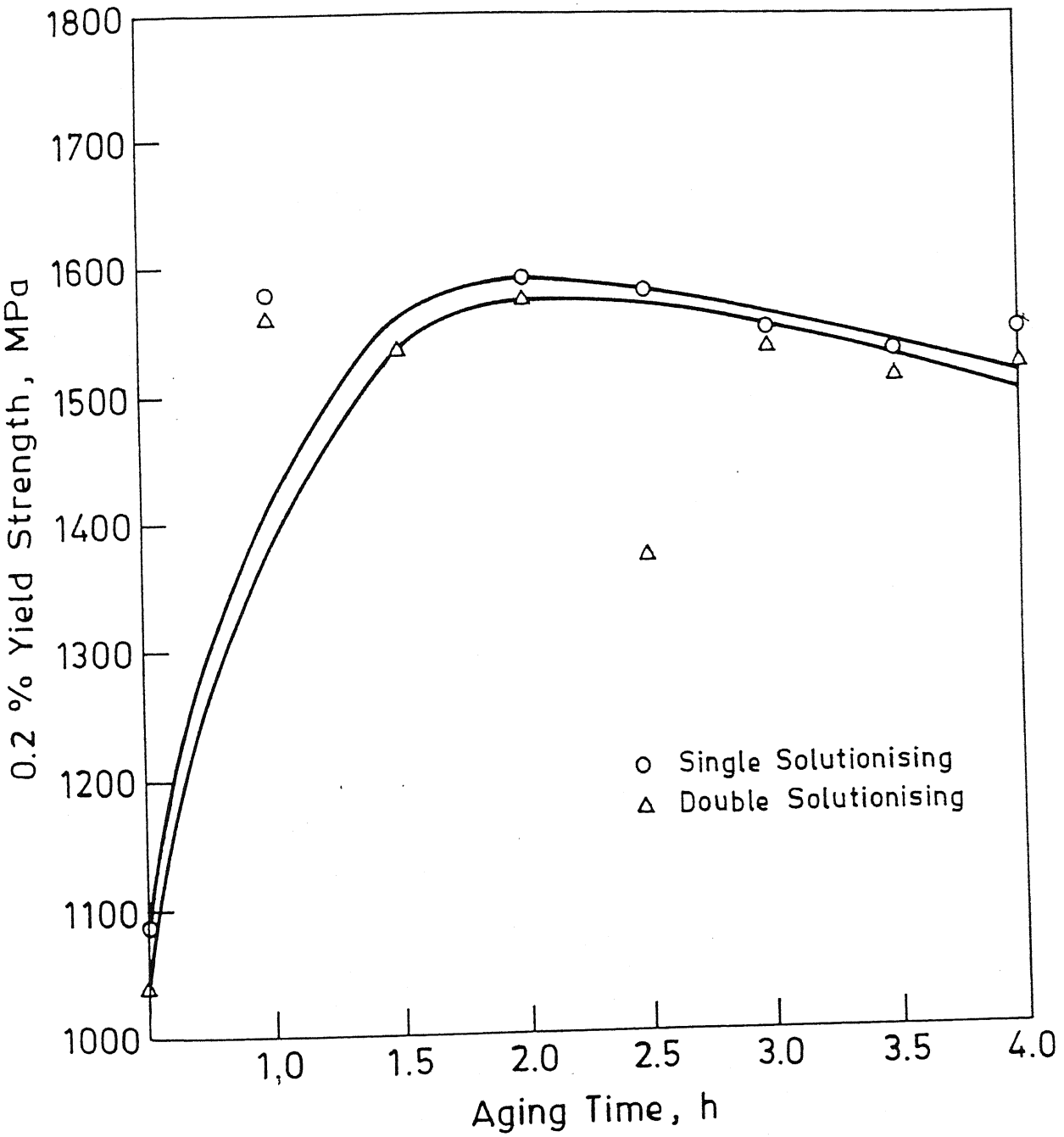

Fig. 4.8. Comparison of the Two Solutionising Treatments at 480 °C.

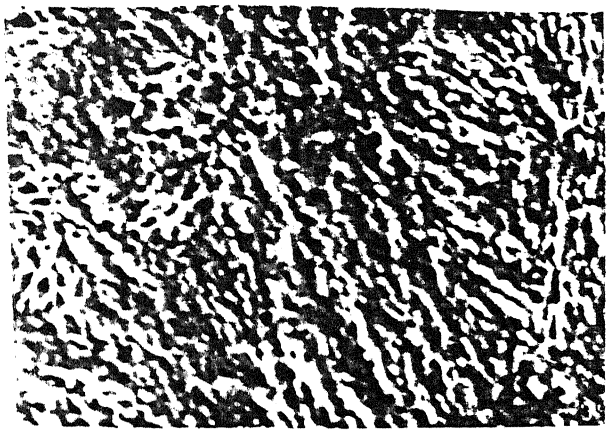

FIG. 4.9

AR, M = 2000X

EE

FIG. 4.10

AR, M = 10,000X

CE

FIG. 4.11

AR+TMT+SS M = 200X

CE

FIG. 4.12

AR+TMT+DS M = 200X

CE

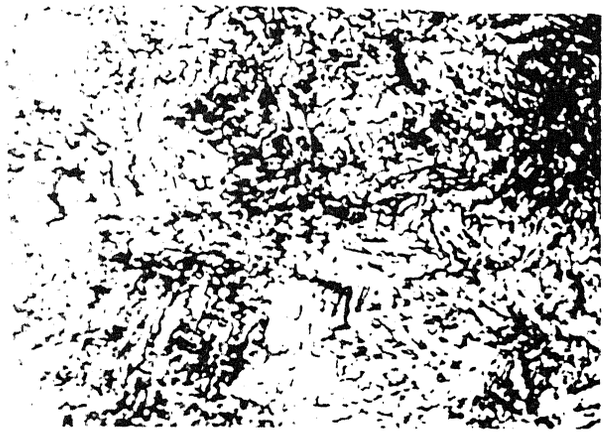

FIG. 4.13

AR M = 1000X

EE

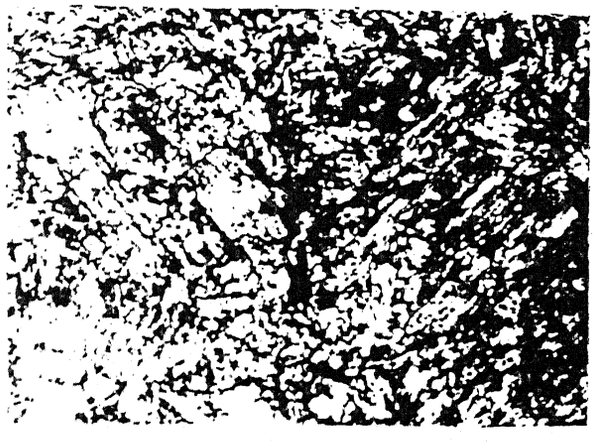

FIG. 4.14

'AR+TMT M = 1000X

EE

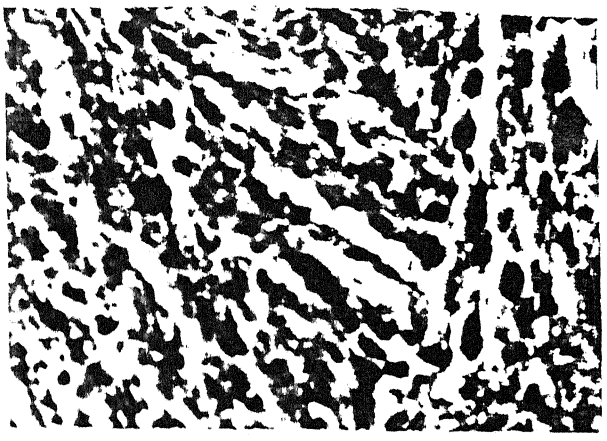

FIG. 4.15

AR M = 5000X

EE

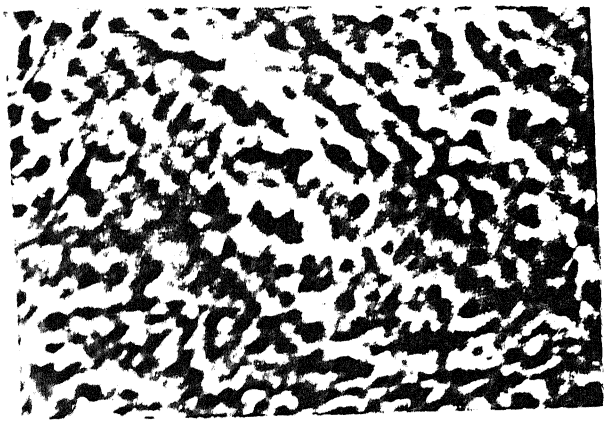

FIG. 4.16

AR+TMT, M = 5000X

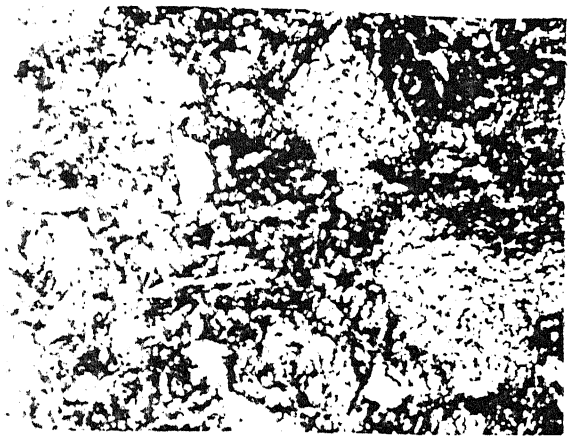

FIG. 4.17

AR+TMT+DS+400,3hrs M = 500X

CE

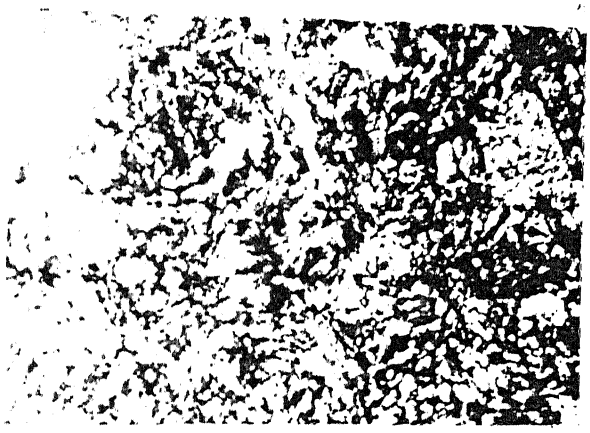

FIG. 4.18

AR+TMT+DS+450,3hrs M = 500X

CE

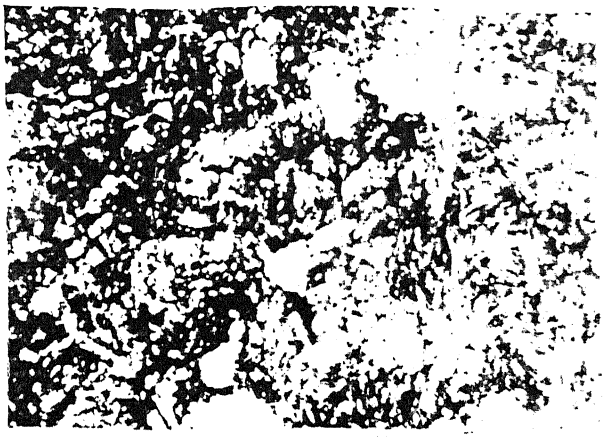

FIG. 4.19

AR+TMT+DS+480,3hrs M = 500X

CE

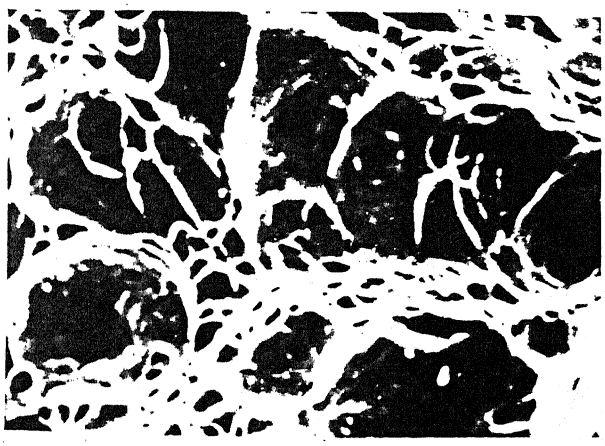

FIG. 4.20

AR+TMT M = 6000X

SEM

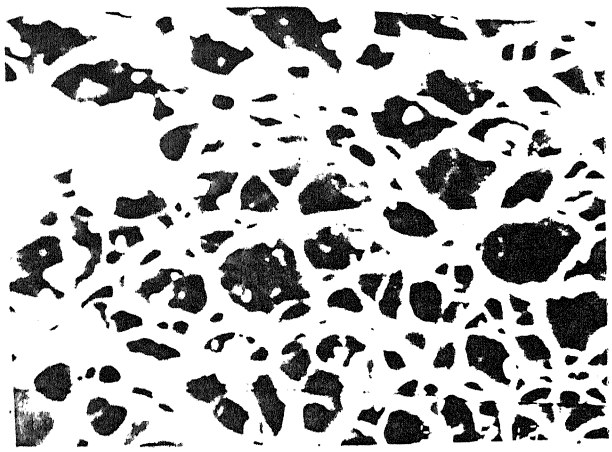

FIG. 4.21

AR+TMT+DS M = 4000X

SEM

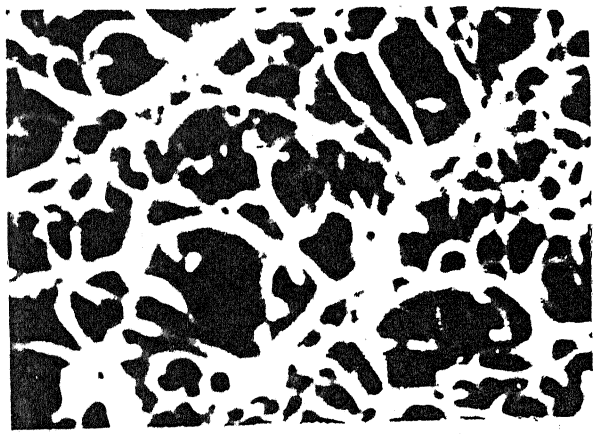

FIG. 4.22

AR+TMT+SS M = 5000X

SEM

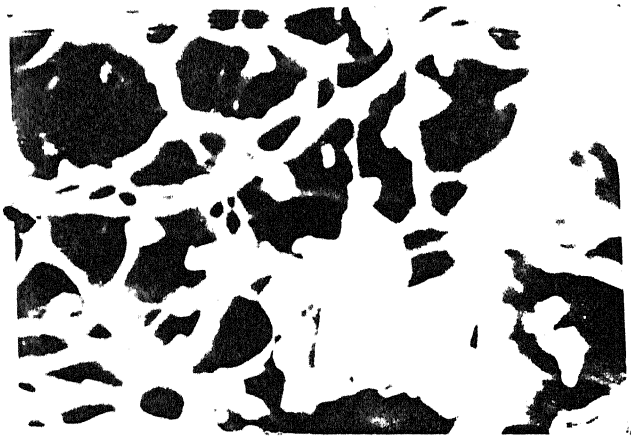

FIG. 4.23

AR+TMT+SS+480,3hrs M = 6000X

SEM

TABLE 4.1

Effect of Aging time on Mechanical Properties of 18 Ni 250 Maraging Steel with Single solutionising and aging at 400°C.

S. No.	Aging Time (h)	Tensile Strength (MPa)	0.2% Yield Strength (MPa)	Elongation Percent (%)	Average Hardness (HV)
1.	0	1082	1082	6.00	328
2.	1.0	1341	1341	5.50	407
3.	1.5	1519	1519	5.25	437
4.	2.0	1477	1477	5.26	474
5.	2.5	1553	1553	5.62	509
6.	3.0	1598	1598	5.37	555
7.	3.5	1670	1670	5.28	557
8.	4.0	1689	1689	5.50	570

TABLE 4.2

Effect of Aging time on Mechanical Properties of 18 Ni 250 Maraging Steel with Single solutionising and aging at 450°C.

S. No.	Aging Time (h)	Tensile Strength (MPa)	0.2% Yield Strength (MPa)	Elongation Percent (%)	Average Hardness (HV)
1.	0	1082	1082	6.00	328
2.	1.0	1553	1553	5.25	455
3.	1.5	1500	1500	5.00	488
4.	2.0	1547	1547	5.08	528
5.	2.5	1578	1578	4.87	549
6.	3.0	1608	1608	4.75	527
7.	3.5	1605	1605	5.01	522
8.	4.0	1624	1624	4.95	555

TABLE 4.3

Effect of Aging time on Mechanical Properties of 18 Ni 250 Maraging Steel with Single solutionising and aging at 480°C.

S. No.	Aging Time (h)	Tensile Strength (MPa)	0.2% Yield Strength (MPa)	Elongation Percent (%)	Average Hardness (HV)
1.	0	1082	1082	6.00	328
2.	1.0	1578	1578	5.17	503
3.	1.5	1555	1555	5.18	526
4.	2.0	1599	1599	4.75	549
5.	2.5	1650	1650	4.50	518
6.	3.0	1541	1541	4.63	514
7.	3.5	1523	1523	4.56	530
8.	4.0	1531	1531	4.62	526

TABLE 4.4

Effect of Aging time on Mechanical Properties of 18 Ni 250 Maraging Steel with Double solutionising and aging at 400°C.

S. No.	Aging Time (hrs)	Tensile Strength (MPa)	0.2% Yield Strength (MPa)	Elongation Percent (%)	Average Hardness (HV)
1.	0	1041	1041	5.90	311
2.	1.0	1308	1308	5.5	395
3.	1.5	1445	1445	5.15	449
4.	2.0	1289	1289	5.0	450
5.	2.5	1546	1546	5.06	489
6.	3.0	1540	1540	5.25	540
7.	3.5	1633	1633	5.17	521
8.	4.0	1671	1671	5.37	560

TABLE 4.5

Effect of Aging time on Mechanical Properties of 18 Ni 250 Maraging Steel with Double solutionising and Aging at 450°C.

S. No.	Aging Time (h)	Tensile Strength (MPa)	0.2% Yield Strength (MPa)	Elongation Percent (%)	Average Hardness (HV)
1.	0	1041	1041	5.90	311
2.	1.0	1553	1553	5.05	438
3.	1.5	1431	1431	5.15	502
4.	2.0	1569	1569	4.75	510
5.	2.5	1633	1633	4.50	562
6.	3.0	1595	1595	4.87	525
7.	3.5	1574	1574	5.00	537
8.	4.0	1625	1625	5.08	526

TABLE 4.6

Effect of Aging time on Mechanical Properties of 18 Ni 250 Maraging Steel with Double solutionising and aging at 480°C.

S. No.	Aging Time (h)	Tensile Strength (MPa)	0.2% Yield Strength (MPa)	Elongation Percent (%)	Average Hardness (HV)
1.	0	1041	1041	5.90	311
2.	1.0	1659	1659	5.17	475
3.	1.5	1537	1537	4.89	524
4.	2.0	1578	1578	4.50	525
5.	2.5	1373	1373	4.41	581
6.	3.0	1527	1527	4.59	563
7.	3.5	1510	1510	4.50	493
8.	4.0	1522	1522	4.62	510

CHAPTER 5

CONCLUSIONS

(1) Both for single and double solutionising at higher aging temperatures ie 480°C high 0.2% yield strength can be attained in a shorter time as compared to lower temperatures ie 400°C. But higher values of 0.2% yield strength are attained at low temperatures when aging is done for longer time whereas at high temperatures 0.2% yield strength goes down for longer aging time.

(2) Behaviour of hardness with change in aging time is similar to that of 0.2% yield strength with change in aging time.

(3) Ductility goes down with increase in aging time at all temperature. Only after substantial aging it begins to rise. Ductility is relatively high at lower aging temperatures.

(4) There is no difference in mechanical properties obtained by single and double solutionising treatments at higher aging temperatures (480°C). This is because of the fact that kinetics of aging are high at higher aging temperatures.

(5) At the aging temperature of 450°C also there is very little difference in mechanical properties of single and double solutionised steels.

(6) At lower temperatures ie 400°C the single solutionised steel attains the desired mechanical properties at a faster rate as compared to double solutionised steel.

(7) The aging reaction at 400°C is considerably lower than that at 480°C, because the kinetics of precipitation hardening is low at lower temperature. For practical applications where

only partial hardening is required so as to get a better combination of strength and toughness, aging at lower temperatures would offer greater control.

(8) Double solutionising gives rise to a coarse microstructure and reduces mechanical properties both in annealed and aged conditions.

(9) Double solutionising does not give any advantage with respect to properties.

(10) Thermomechanical treatment refines the lath width of 18Ni 250 maraging steel.

(11) Intercrystalline brittle fracture takes place in 18Ni 250 maraging steel.

REFERENCES

1. B.Z. Weiss, "Speciality Steels and Hard Materials", Proc. of the International Conference on Recent Developments in Speciality Steels and Hard Materials (edited by N.R. Comins and J.B. Clark) p.35, Pergamon Press (1982).
2. R.F. Decker, C.J. Novak and T.W. Landig, Journal of Metals, 11, 60 (1967).
3. S. Floreen, Met. Reviews, 13, 115 (1968).
4. F.W. Zones and W.I. Pumphrey, Jour. Iron Steel Inst., 163, 121 (1949).
5. J.M. Marder and A.R. Marder, Trans. ASM, 62, 1 (1969).
6. T. Maki, K. Tsuzaki and I. Tamura, Tetsu-to-Hagané, 65, 515 (1979).
7. V.D. Sadovskiy, V.M. Schastlivtsev, Yu.V. Kaletina and I.L. Yakoleva, Phys. Met. Metallog., 62, 190 (1986).
8. C. Servant and G. Cizeron, Mém. Sci. Rev. Mét, 66, 531 (1969).
9. K. Hosomi, Y. Ashida, H. Hato and K. Ishihara, Tetsu-to-Hagané, 61, 1012 (1975).
10. T. Fujita, K. Asami, S. Yamamoto and H. Tutumi, Tetsu-to-Hagané, 56, 214 (1970).
11. V.D. Sadovskiy, Phys. Met. Metallog., 57, 1 (1984).
12. G. Krauss and M. Cohen, Trans. AIME, 224, 1212 (1962).
13. T.J. Koppenaal and E. Gold, Met. Trans. 3, 2965 (1972).
14. G.P. Miller and W.I. Mitchell, Jour. Iron Steel Inst., 203, 899 (1965).

15. J.M. Chilton and C.J. Barton, Trans. ASM, 60, 528 (1967).

16. S.K. Das and G. Thomas, Trans. ASM, 62, 659 (1969).

17. R.D. Garwood and R.D. Jones, Jour. Iron Steel Inst., 204, 512 (1966).

18. S. Takaki and Y. Tokunaga, Trans. JIM, 23, 31 (1982).

19. A.F. Yedneral, O.P. Zhukov, M.A. Kablukovskaya, B.M. Mogutnov and M.D. Perkas, Phys. Met. Metallog., 36, 46 (1973).

20. D.T. Peters and C.R. Cupp, Trans. Met. Soc. AIME, 236, 1420 (1966).

21. J.M. Genin and G. LeCaer, Scripta Met., 8, 15 (1974).

22. C. Servant, G. Maeder and G. Cizeron, Met. Trans., 6A, 981 (1981).

23. Y. Tokunaga and M. Morishige, J. Japan Inst. Metls, 43, 834 (1979).

24. H. Ohtani, F. Teraski and T. Kunitake, Tetsu-to-Hagané, 58, 434 (1972).

25. A.R. Harder and G. Krauss, Trans. ASM, 62, 957 (1969).

26. M.J. Roberts, Met. Trans., 1, 3287 (1970).

27. T. Swarr and G. Krauss, Met. Trans., 7A, 41 (1976).

28. L.-Å. Norström, Scand. J. Met., 5, 41 (1976).

29. K. Hosumi, Y. Ashida, H. Hato and K. Ishihara, Tetsu-to-Hagané, 64, 1047 (1978).

30. L.-Å. Norström, Metal Sci. J., 10, 429 (1976).

31. S. Matsuda, T. Inoue, H. Mimura and Y. Okamoto, Proc. of Inter. Sympo. on Toward Improved Ductility and Toughness, Climax Molybdenum Development Co. (Japan) Ltd., 47 (1971).

32. W.S. Owen, Proc. of 2nd Inter. Conf. on Strength of Metals and Alloys, III, Asilomar, 795 (1970).

33. Y. Kawabe, K. Nakazawa and S. Muneki, Trans. Nat. Research Inst. Metals, 20, 229 (1978).

34. S. Muneki, Y. Kawabe and K. Nakazawa, Tetsu-to-Hagané, 64, 605 (1978).

35. R.W. Hayes, Materials Science and Technology, 1, 285 (1985).

36. P. Rodriguez, Bulletin of Materials Science, 6, 653 (1984).

37. J.C. Fisher, Acta Metall, 2, 9 (1954).

38. G. Schoeck and A. Seeger, Acta Metall, 7, 469 (1959).

39. S.L. Mannan and P. Rodriguez, Phil. Mag, 25, 673 (1972).

40. G.E. Dieter, "Mechanical Metallurgy", Third Edition, pp 284-297, McGraw-Hill Book Company, (1986).

41. R.W. Hayes and W.C. Hayes, Acta Metall., 30, 1295 (1982).

42. R.W. Hayes, Acta Metall., 31, 365 (1983).

43. R.W. Hayes and W.C. Hayes, Acta Metall., 32, 259 (1984).

44. L.P. Kubin and Y. Estrin, Acta Metall. Mater., 38, 697 (1990).

45. A. Van den Beukel, Physica Status Solidi(a) 30, 197 (1975).

46. D.M. Barnett, W.C. Oliver and W.C. Nix, Acta Metall., 30, 673 (1982).

47. A.H. Cottrell, "Dislocations and plastic flow in crystals", pp.147-149, Clarendon Press, Oxford, (1953).

48. P.G. McCormick, Acta Metall., 36, 3061 (1988).

49. W. Räuchle, O. Vöhringer and E. Macherauch, Mater. Sci. Engng, 12, 147 (1973).

50. H. Conrad and H. Weidersich, Acta Metall., 8, 128 (1960).

51. Z.S. Basinski, Acta Metall., 5, 684 (1957).

52. T. Nakada and A.S. Keh, Acta Metall., 18, 437 (1970).

53. R.A. Mulford and U.F. Kocks, Acta Metall., 27, 1125 (1979).

54. S.G. Harris, "Vacancies and other point defects in metals and alloys", (1st Edn), pp 220-221, Bungay, Suffolk, Richard Clay and Co. (1958).

SUGGESTIONS FOR FURTHER WORK

(1) Aging at lower temperatures can be done which is expected to give more ductility.

(2) Creep test of the material could be done.

(3) Aging for longer times can also be done.

(4) We can also do tensile testing of the material in directions other than the rolling direction like 45° to the rolling direction, 90° to the rolling direction etc.

(5) Transmission electron microscopy of the aged samples could shed more light on the process of aging.